

Torsion and shear stresses due to shear centre eccentricity
in SCIA Engineer
Delft University of Technology

Marijn Drillenburg

October 2017

Contents

| | | |
|----------|--|-----------|
| 1 | Introduction | 2 |
| 1.1 | Hand Calculation | 2 |
| 1.2 | Results in SCIA | 4 |
| 2 | Investigation Plan | 6 |
| 3 | Geometry | 7 |
| 3.1 | I-shaped cross section | 7 |
| 3.2 | L-shaped cross section | 8 |
| 3.3 | Findings | 10 |
| 4 | Boundary Conditions | 11 |
| 4.1 | Cantilever Beam | 11 |
| 4.2 | Double clamped beam | 13 |
| 4.3 | Findings | 15 |
| 5 | Loading | 16 |
| 5.1 | Pure bending | 16 |
| 5.2 | Point load in normal force centre | 18 |
| 5.3 | Point load in shear centre | 20 |
| 5.4 | Findings | 22 |
| 6 | Conclusion | 23 |
| 6.1 | Geometry | 23 |
| 6.2 | Boundary Conditions | 24 |
| 6.3 | Loading | 24 |
| 7 | Recommendations | 26 |
| | Appendices | 28 |
| A | Torsion Theory | 29 |
| B | Framework Analysis | 34 |
| B.1 | Overview | 34 |
| B.2 | Generation of input file | 34 |
| B.3 | The Kernel | 37 |
| B.4 | GUI | 39 |
| C | Maple Files | 42 |
| C.1 | Cross sectional properties | 42 |
| C.2 | L-shaped cross section loaded in pure bending | 45 |
| C.3 | L-shaped cross section loaded in normal force centre | 48 |

Chapter 1

Introduction

There is a suspicion that the framework analysis program “SCIA Engineer” is not computing torsional stresses and deformations in the correct way. To illustrate how this suspicion came to light, this chapter provides the reader with an example structure in which torsion occurs. The structure will be analysed theoretically first, by doing a hand calculation using the theory described in Appendix A. This calculation will produce expected stress values. These expectations will be compared to results from an analysis of the structure in SCIA Engineer. Based on these results, a plan will be presented to further analyse the possible problems.

1.1 Hand Calculation

We will first focus on a double clamped beam, loaded with point load in the normal force centre at a distance “ l_1 ” on the span. The cross section is L-shaped and pictured in Figure 1.2. Since this cross section is not symmetrical, we know from Appendix A this type of loading will not only cause bending moments, but also a torsional moment. This is caused by shear centre eccentricity in the non-symmetrical cross section. A schematic drawing of the structure is displayed in Figure 1.1.

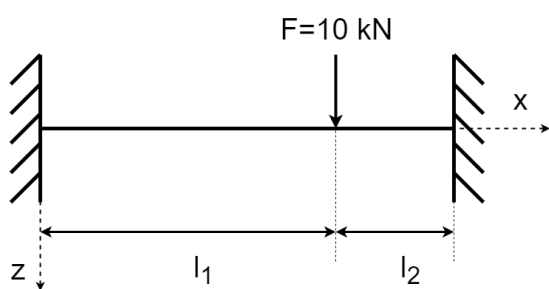


Figure 1.1: Double clamped beam with torsional moment

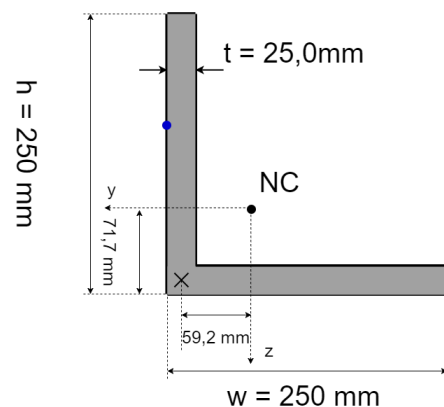


Figure 1.2: L-shaped Cross Section

Table 1.1: Material Properties

| | Symbol | S235 |
|-----------------|--------|---------------------------------|
| Young's modulus | E | $210 \cdot 10^3 \text{ N/mm}^2$ |
| Shear modulus | G | $8.1 \cdot 10^4 \text{ N/mm}^2$ |

The location of the normal force centre and the shear force centre have already been computed. This calculation was done by hand at first. Then the calculation was done again in Maple. The calculation in Maple yielded the same results. To save time, from now on Maple is used for the calculations. A Maple file where the properties for this cross section are calculated is attached under the section “L-shaped” in Appendix C.1. For this example, we are interested in the internal torsional moments in the two parts of the beam. We name the torsional moment caused by eccentricity of the point load “T”. If we solve this structure in terms of T, l_1 , l_2 and the cross sectional properties, we can later vary the different parameters easily and consider different positions for the load. Because this is a static indeterminate structure, we can not simply solve this problem using equilibrium. We need an additional equation. In this example we use the fact that the rotation φ_{x1} just left of the applied moment has to be equal to the rotation φ_{x2} just to the right. First we divide the beam into two parts, as shown in Figure 1.3.

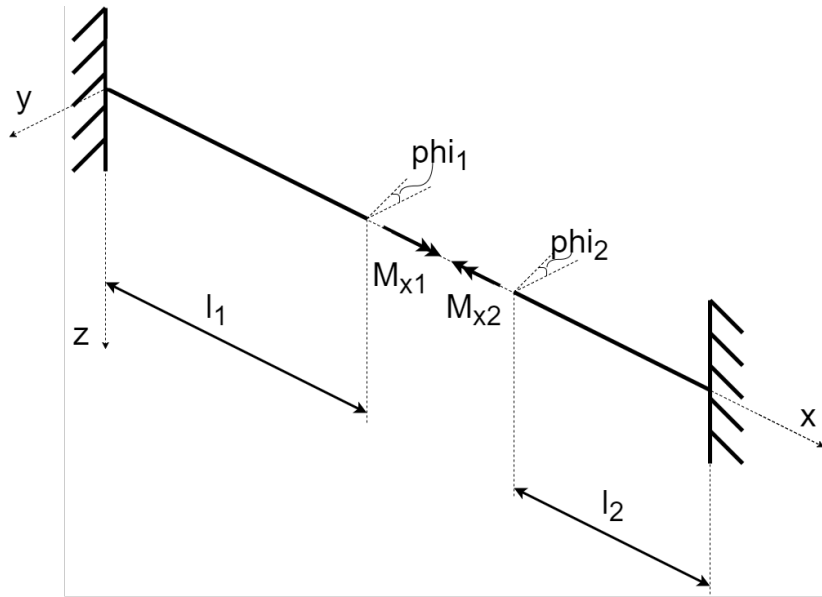


Figure 1.3: Double clamped beam divided in two parts

The assumed moments M_{x1} and M_{x2} , and the externally applied torque T have to satisfy the equilibrium equation where the total moment around the node is 0. This leads to the first equation:

$$T + M_{x1} - M_{x2} = 0 \quad (1.1)$$

We already know the constitutive relation between externally applied torque and rotation of a cross section. The second equation becomes:

$$\begin{aligned} \varphi_{x1} &= \varphi_{x2} \\ \frac{M_{x1} \cdot l_1}{GI_t} &= \frac{M_{x2} \cdot l_2}{GI_t} \end{aligned} \quad (1.2)$$

Solving for the unknown moments yields

$$\begin{aligned} M_{x1} &= T \cdot \frac{l_2}{l_1 + l_2} \\ M_{x2} &= -T \cdot \frac{l_1}{l_1 + l_2} \end{aligned} \quad (1.3)$$

This leads to the moment distribution as shown in Figure 1.4. From these results it can be concluded that in a situation where a beam is loaded in torsion somewhere along the span,

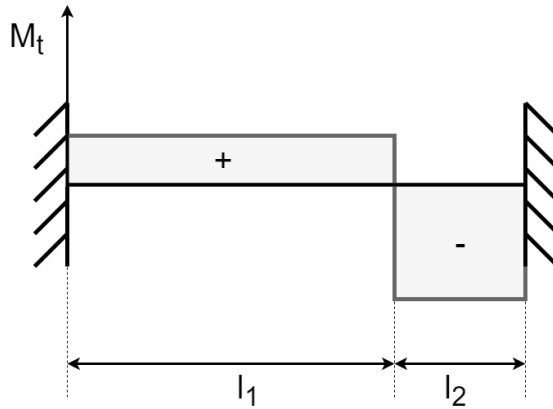


Figure 1.4: Moment distribution of double clamped beam

the distribution of the torsional moment can be determined by the equations from (1.3). The shear stresses that will occur are linear in M_t , so they will also follow this distribution. We will consider three load cases:

- Load at midspan
- Load at 1/4 span
- Load at 1/10 span

For each of these load cases, we will determine the expected shear stresses and compare them to the results in SCIA. The computation of the cross sectional properties and torsional moment can be found in the Maple-file in Appendix C.1. We recall the theory for thin walled open elements from Appendix A, and fill in equation (A.11) to find the maximum shear stress in the cross section:

$$\tau_{max} = \frac{M_t \cdot s_c}{\frac{1}{2}I_t} = \frac{0.592 \cdot 10^6 \text{Nmm} \cdot \frac{t}{2}}{\frac{1}{2} \cdot 2.47 \cdot 10^6 \text{mm}^4} = 5.98 \text{N/mm}^2 \quad (1.4)$$

Now we can scale this maximum value to the different load scenarios, using the formulas from equation (1.3). The expected shear stresses are now known, and are reported in table 1.2. Note that τ_1 represents the maximum shear stress left of where the load is applied and τ_2 represents the maximum shear stress on the right.

Table 1.2: Expected shear stresses

| | τ_1 [%] | τ_1 [N/mm ²] | τ_2 [%] | τ_2 [N/mm ²] |
|-------------------|--------------|-------------------------------|--------------|-------------------------------|
| Load at midspan | 50% | 2.99 | 50% | -2.99 |
| Load at 1/4 span | 75% | 4.49 | 25% | -1.50 |
| Load at 1/10 span | 90% | 5.39 | 10% | -0.60 |

1.2 Results in SCIA

The structure is now imported in SCIA using the dimensions and material properties defined above. The shear stresses are evaluated for every load scenario presented in the former section. In SCIA we have to choose in which fibre the shear stress has to be displayed. Fibre 14 is chosen. This fibre is shown as a blue dot in Figure 1.2. The values for the shear stress are reported in the bold column labeled “ τ_{xy}/τ_{xs} ”.

| ▲ | Name | dx [m] | Fibre | Case | σ_x [MPa] | τ_{xy} / τ_{xs} [MPa] | τ_{xz} / τ_{zs} [MPa] |
|---|------|--------|---------|-----------------|------------------|-------------------------------|-------------------------------|
| 1 | B1 | 0,000 | Fibre14 | Load at midspan | 4,00361 | 4,24264 | 0,62177 |
| 2 | B1 | 2,500- | Fibre14 | Load at midspan | -4,00362 | 4,24264 | 0,62177 |
| 3 | B1 | 2,500+ | Fibre14 | Load at midspan | -4,00362 | -4,24264 | -0,62177 |
| 4 | B1 | 5,000 | Fibre14 | Load at midspan | 4,00361 | -4,24264 | -0,62177 |

Figure 1.5: Stress results with load at midspan

| ▲ | Name | dx [m] | Fibre | Case | σ_x [MPa] | τ_{xy} / τ_{xs} [MPa] | τ_{xz} / τ_{zs} [MPa] |
|---|------|--------|---------|------------------|------------------|-------------------------------|-------------------------------|
| 1 | B1 | 0,000 | Fibre14 | Load at 1/4 span | 4,48320 | 7,15338 | 1,04823 |
| 2 | B1 | 0,500- | Fibre14 | Load at 1/4 span | 1,78493 | 7,15338 | 1,04823 |
| 3 | B1 | 0,500+ | Fibre14 | Load at 1/4 span | 1,78493 | 7,15338 | 1,04823 |
| 4 | B1 | 1,250- | Fibre14 | Load at 1/4 span | -2,26247 | 7,15338 | 1,04823 |
| 5 | B1 | 1,250+ | Fibre14 | Load at 1/4 span | -2,26247 | -1,33190 | -0,19532 |
| 6 | B1 | 5,000 | Fibre14 | Load at 1/4 span | 1,52222 | -1,33190 | -0,19532 |

Figure 1.6: Stress results with load at 1/4 span

| ▲ | Name | dx [m] | Fibre | Case | σ_x [MPa] | τ_{xy} / τ_{xs} [MPa] | τ_{xz} / τ_{zs} [MPa] |
|---|------|--------|---------|-------------------|------------------|-------------------------------|-------------------------------|
| 1 | B1 | 0,000 | Fibre14 | Load at 1/10 span | 2,57832 | 8,24303 | 1,20795 |
| 2 | B1 | 0,500- | Fibre14 | Load at 1/10 span | -0,53169 | 8,24303 | 1,20795 |
| 3 | B1 | 0,500+ | Fibre14 | Load at 1/10 span | -0,53169 | -0,24225 | -0,03560 |
| 4 | B1 | 1,250- | Fibre14 | Load at 1/10 span | -0,39236 | -0,24225 | -0,03560 |
| 5 | B1 | 1,250+ | Fibre14 | Load at 1/10 span | -0,39236 | -0,24225 | -0,03560 |
| 6 | B1 | 5,000 | Fibre14 | Load at 1/10 span | 0,30429 | -0,24225 | -0,03560 |

Figure 1.7: Stress results with load at 1/10 span

A comparison between the theory and the results from SCIA is presented in table 1.3. It can be observed that none of the values from SCIA correspond to their expected value. In most cases the value in SCIA is higher. In two of the cases, the value reported in SCIA is lower than the expected value. For example, the τ_2 for the load at 1/10 span is 60% lower than the expectation.

Table 1.3: Comparison between theory and SCIA

| | $\tau_{1,exp}$ [N/mm ²] | $\tau_{1,scia}$ [N/mm ²] | Diff | $\tau_{2,exp}$ [N/mm ²] | $\tau_{2,scia}$ [N/mm ²] | Diff |
|-------------------|--|---|--------|--|---|--------|
| Load at midspan | 2.99 | 4.24 | +41.8% | 2.99 | 4.24 | +41.8% |
| Load at 1/4 span | 4.49 | 7.15 | +59.2% | 1.50 | 1.33 | -11.3% |
| Load at 1/10 span | 5.39 | 8.24 | +52.8% | 0.60 | 0.24 | -60.0% |

When considering engineering purposes, this discrepancy can lead to dangerous situations. If the shear stresses occurring in a structure are 60% higher than their expected value, safety may not be guaranteed. Therefore it should be investigated why the values in SCIA do not correspond with the theory.

Chapter 2

Investigation Plan

To investigate why SCIA is not displaying the values as we would expect, the following plan is presented to eliminate potential issues.

The first factor we will consider is the geometry of the cross section. Without considering loading or boundary conditions, the cross sectional properties for various shapes will be analysed. Important steps in this process are the determination of the normal force centre and the shear force centre. The calculation will be done by hand at first, while comparing it to the values observed in SCIA later. This check will eliminate issues with the geometry, which can cause wrong results of the torsion calculation.

The second variable we will check for issues are the boundary conditions. For a simple loading scenario, we will analyse different boundaries. Again we will first calculate the values by hand. Then a calculation in SCIA is performed, and the two results will be compared. This check will determine whether the torsional deformation and stress results for a basic example are in line with the theory. Another goal of this section is to check whether the distribution of the internal torsional moment is performed correctly in SCIA.

The final parameter we will check is the loading. In this part of the investigation we will consider different loading situations. While we keep the cross section and boundary conditions fixed, we will vary the loading type and check for differences between a hand calculation and the results from SCIA. This check will provide insight in whether the type of loading influences the torsion results.

By following the steps described in this investigation strategy, answers can be formulated to the following questions:

- Does SCIA calculate cross sectional properties in the correct way?
- Do different boundary conditions influence the torsion results in SCIA?
- Is the discrepancy between the theory and SCIA influenced by varying the loading?

These answers will provide the reader with a better understanding of the source of the problem with the torsion calculation. After the different aspects of this problem are investigated, the logical next step is to start thinking about solutions to the potential issue. To begin this thought process, it is important to have a better understanding of how the software package operates. Therefore research is performed on frame analysis software in general. This will be done by means of considering a very simple example of a framework structure, for which a program is written to solve the internal force distribution and the deflections. After this procedure, the issues in the program can possibly be explained. This leads to the final question:

- Can an advice be formulated to the developers of SCIA Engineer to reduce discrepancy in value between a theoretical approach and an analysis in SCIA of a torsion calculation?

Chapter 3

Geometry

Determining the characteristics of the cross section is one of the first steps SCIA takes in the evaluation process. This procedure is performed in the Graphical User Interface, as described in Appendix B. An issue here could cause wrong results in a stress calculation, so it makes sense to investigate whether the values produced in SCIA are correct. To eliminate an issue with the calculation of the cross sectional properties we will calculate various cross sections by hand first, and compare them to the values obtained from SCIA. The manual provided by SCIA (Section on determination of standardised cross sectional properties) provides us with the solution strategy. The cross sectional properties are determined in two parts. The values that are calculated in these two parts are:

- Part I: Biaxial bending and axial force
 - Area
 - Centre of gravity
 - Angle of the principal axis system
 - Principle moments of inertia
- Part II: Torsion
 - Shear Centre
 - Torsional moment of inertia
 - Warping constant
 - Warping ordinate

A good strategy to check whether the Part I properties are correct, is comparing the moments of inertia I_{yy} , I_{zz} and I_{yz} for each cross section. Since determining the warping constant and the warping ordinate both are outside the scope of this paper, we will focus on finding the position of the shear centre and the magnitude of the torsional moment of inertia when investigating the Part II information. We will consider two different cross section types:

- Symmetrical in two axes
- Symmetrical in one axis

As mentioned before, for each type a comparison between the theory and the values from SCIA will be made. If the values correspond to their expected value, we can eliminate an issue here. If the values do not correspond, further investigation is necessary.

3.1 I-shaped cross section

The first cross section type we will consider is a double symmetrical I-shaped section. The shape and dimensions are presented in Figure 3.1. Since this cross section is symmetrical in two axes, we know the shear centre should coincide with the normal force centre. We also expect to see a zero magnitude of I_{yz} , due to symmetry. The calculation of the cross sectional properties is

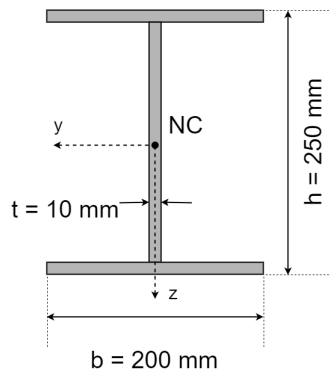
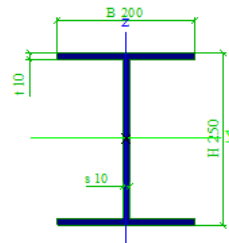


Figure 3.1: I-shaped cross section

performed in Maple, for checking this calculation a reference is made to Appendix C.1. The results from SCIA can be observed in Figure 3.2. A comparison between these results is made in table 3.1. As can be observed from this table, the values in SCIA show no discrepancies with the results from the theory.

| | | |
|------------------------------|---------------------|--|
| Name | I-shaped | |
| Type | I | |
| Detailed | 250; 200; 10; 10; 0 | |
| Item material | S235 | |
| Fabrication | rolled | |
| Flexural buckling y-y | a | |
| Flexural buckling z-z | b | |
| Use 2D FEM analysis | x | |



| | | |
|---|------------|------------|
| A [mm²] | 6,3000e+03 | |
| A y, z [mm²] | 3,6567e+03 | 2,5112e+03 |
| I y, z [mm⁴] | 6,7773e+07 | 1,3353e+07 |
| I w [mm⁵], t [mm⁴] | 1,9200e+11 | 2,1304e+05 |
| Wey, z [mm³] | 5,4218e+05 | 1,3353e+05 |
| Wply, z [mm³] | 6,1225e+05 | 2,0575e+05 |
| d y, z [mm] | 0 | 0 |
| c YUCS, ZUCS [mm] | 100 | 125 |
| α [deg] | 0,00 | |
| A L, D [mm²/mm] | 1,2798e+03 | 1,2798e+03 |
| Mply +, - [Nmm] | 1,44e+08 | 1,44e+08 |
| Mplz +, - [Nmm] | 4,84e+07 | 4,84e+07 |

Figure 3.2: Cross sectional properties of I-shaped in SCIA

3.2 L-shaped cross section

Now we will consider a cross section that has only one axis of symmetry. The location of the shear centre will therefore not coincide with the normal force centre. The cross section we will discuss is L-shaped, and has dimensions as pictured in Figure 3.3. Again the cross section is first

Table 3.1: Comparison theory and SCIA for I-shaped cross section

| | | Expectation | SCIA |
|-----------------------------|----------------------|-----------------------------------|-----------------------------------|
| Centroid | (y_{nc}, z_{nc}) | (100mm,125mm) | (100mm,125mm) |
| Area | A | 6300 mm ² | 6300 mm ² |
| Moment of inertia y-axis | I_{yy} | $6.78 \cdot 10^7$ mm ⁴ | $6.78 \cdot 10^7$ mm ⁴ |
| Moment of inertia z-axis | I_{zz} | $1.34 \cdot 10^7$ mm ⁴ | $1.34 \cdot 10^7$ mm ⁴ |
| Moment of inertia combined | I_{yz} | 0 | 0 |
| Torsional moment of inertia | I_t | $2.13 \cdot 10^5$ mm ⁴ | $2.13 \cdot 10^5$ mm ⁴ |
| Eccentricity Shear Centre | (dy,dz) | (0,0) | (0,0) |

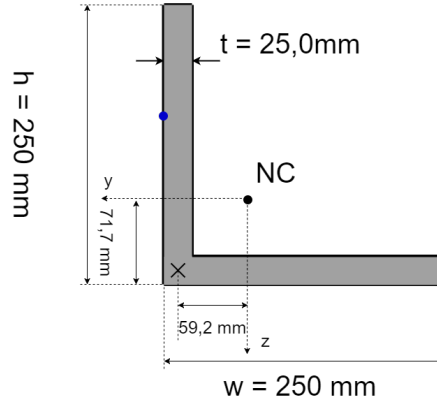


Figure 3.3: L-shaped cross section

analysed by hand. This hand calculation is reported in the form of a Maple-file in Appendix C.1. The location of the shear centre is determined using the theory that for thin-walled L-shaped cross sections, the shear centre lies on the connection between the two flanges(par. 5.5, Toegepaste Mechanica deel 2, Hartsuijker 2003)[1]. Because the eccentricity of the shear centre with respect to the normal force centre is given in the principal coordinate system in SCIA, we have to make an additional calculation. From “Introduction into Continuum Mechanics”[2] we know the transformation rule for rotating coordinate axes:

$$\begin{bmatrix} y_{new} \\ z_{new} \end{bmatrix} = \begin{bmatrix} \cos(\alpha) & \sin(\alpha) \\ -\sin(\alpha) & \cos(\alpha) \end{bmatrix} \cdot \begin{bmatrix} y_{old} \\ z_{old} \end{bmatrix} \quad (3.1)$$

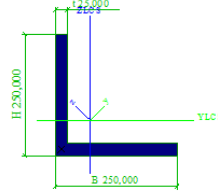
Using these facts the theoretical results are obtained. The cross section is also generated in SCIA, the results from that calculation can be seen in Figure 3.4. Now the values can be compared in Table 3.2.

Table 3.2: Comparison between results from the theory and SCIA for an L-shaped cross section

| | | Expectation | SCIA |
|-----------------------------|----------------------|------------------------------------|------------------------------------|
| Centroid | (y_{nc}, z_{nc}) | (71.71mm,71.71mm) | (71.71mm,71.71mm) |
| Area | A | 11875 mm ² | 11875 mm ² |
| Moment of inertia y-axis | I_{yy} | $7.03 \cdot 10^7$ mm ⁴ | $7.03 \cdot 10^7$ mm ⁴ |
| Moment of inertia z-axis | I_{zz} | $7.03 \cdot 10^7$ mm ⁴ | $7.03 \cdot 10^7$ mm ⁴ |
| Moment of inertia combined | I_{yz} | $-4.16 \cdot 10^7$ mm ⁴ | $-4.16 \cdot 10^7$ mm ⁴ |
| Torsional moment of inertia | I_t | $2.47 \cdot 10^6$ mm ⁴ | $2.47 \cdot 10^6$ mm ⁴ |
| Eccentricity Shear Centre | (dy,dz) | (83.74mm,0) | (83.97mm,0) |

From Table 3.2 it can be concluded that all Part I information is accurate. However, the shear centre eccentricity is not the same as we have calculated by hand and shows a small discrepancy. The difference in value is 0.23 mm.

| | | |
|-----------------------|--|--|
| Name | L-shaped | |
| Type | Angle | |
| Detailed | 250,000; 250,000; 25,000; 0,100; 0,100 | |
| Item material | S235 | |
| Fabrication | rolled | |
| Flexural buckling y-y | c | |
| Flexural buckling z-z | c | |
| Use 2D FEM analysis | x | |



| | | |
|--|-------------|------------|
| A [mm ²] | 1,1875e+04 | |
| A y, z [mm ²] | 1,0116e+04 | 9,9127e+03 |
| I y, z [mm ⁴] | 1,1195e+08 | 2,8682e+07 |
| I YLCS, ZLCS [mm ⁴] | 7,0314e+07 | 7,0314e+07 |
| I w [mm ⁵], t [mm ⁴] | 2,3823e-19 | 2,4740e+06 |
| W _{el} y, z [mm ³] | 6,3327e+05 | 2,8282e+05 |
| W _{pl} y, z [mm ³] | 9,9805e+05 | 5,0317e+05 |
| d y, z [mm] | -83,969 | 0,000 |
| c YUCS, ZUCS [mm] | 71,710 | 71,710 |
| α [deg] | 45,00 | |
| IYZLCS [mm ⁴] | -4,1632e+07 | |
| A L, D [mm ² /mm] | 9,9987e+02 | 9,9987e+02 |
| M _{ply} +, - [Nmm] | 2,35e+08 | 2,35e+08 |
| M _{piz} +, - [Nmm] | 1,18e+08 | 1,18e+08 |

Figure 3.4: Cross sectional properties of L-shaped in SCIA

3.3 Findings

In this chapter we have analysed two types of cross sections:

- Symmetrical in two axes
- Symmetrical in one axis

The values obtained by making a hand calculation have been compared to the result from a calculation in SCIA. In section 3.1 we have established that for cross sections that are symmetrical in two axes, the results in SCIA match the theoretical expectation. In section 3.2, an analysis was made on an L-shaped cross section. This type of cross section is only symmetrical in one axis, which means the shear centre does not coincide with the normal force centre. We observed that the values of most cross sectional properties matched the results in SCIA. However, the shear centre eccentricity reported in SCIA differed from the expectation by 0.23 mm. Further investigation is necessary to find out where this discrepancy originates.

Chapter 4

Boundary Conditions

This chapter investigates the influence of different boundary conditions on the results for torsion analysis. In order to do this, a simple loading scenario is assumed. The L-shaped cross section from Section 3.2 is used. Since we are interested in reviewing the torsional deformation and shear stresses caused by torsion, a torsional moment M_t around the x-axis is applied. A beam element with constant length is then analysed for two different boundary conditions. The first boundary condition that will be considered, is a simple fixed boundary. This type of structure is also known as a cantilever beam. This exercise will establish whether SCIA calculates shear deformation and shear stresses in a basic torsion problem as we would expect. After this check has been carried out, we will focus on an example where the same beam is clamped on both ends. This will lead to a double clamped structure. With that structure, we will be able to determine whether the torsional moment is divided correctly over the beam, and also whether the shear stresses have the same magnitude as we would expect.

4.1 Cantilever Beam

The first example that will be discussed is a single clamped cantilever beam. The cross section is L-shaped, and the structure is loaded with a moment $M_t = 5.0\text{kN}$ around the x-axis. A schematic overview of the structure is presented in Figure 5.1.

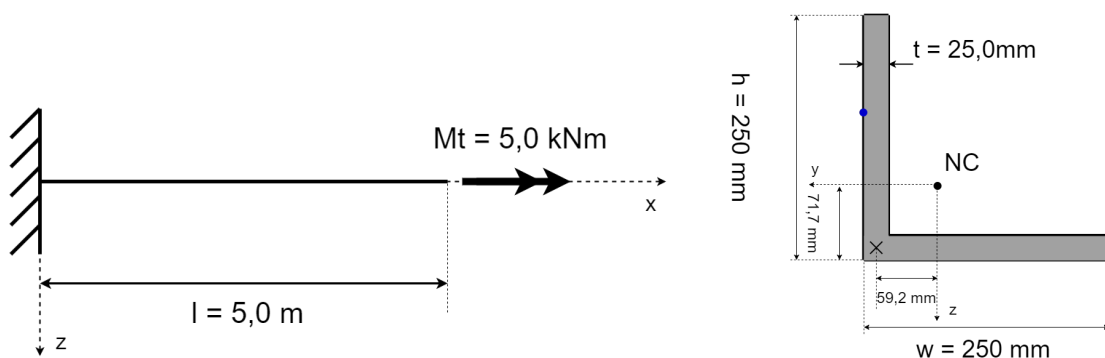


Figure 4.1: Cantilever beam with L-shaped cross-section

Since the cross sectional properties have already been determined in Section 3.2, we can now calculate the maximum shear stress τ_{max} and torsional deformation φ_x using the formulas from

Appendix A:

$$\tau_{max} = \frac{5.0 \cdot 10^6 \text{Nmm} \cdot 12.5 \text{mm}}{0.5 \cdot 2.47 \cdot 10^6 \text{mm}^4} = 50.526 \text{N/mm}^2$$

$$\varphi_x = \frac{5.0 \cdot 10^6 \text{Nmm} \cdot 5000 \text{mm}}{8.1 \cdot 10^4 \text{N/mm}^2 \cdot 2.47 \cdot 10^6 \text{mm}^4} = 124.75 \text{mrad}$$
(4.1)

Now the expected values are known, we can focus on the results from SCIA. The geometry and cross section of the structure are imported, and a calculation is performed. The maximum shear stress and torsional deformation according to SCIA are displayed in Figure 4.3 and Figure 4.4 respectively.

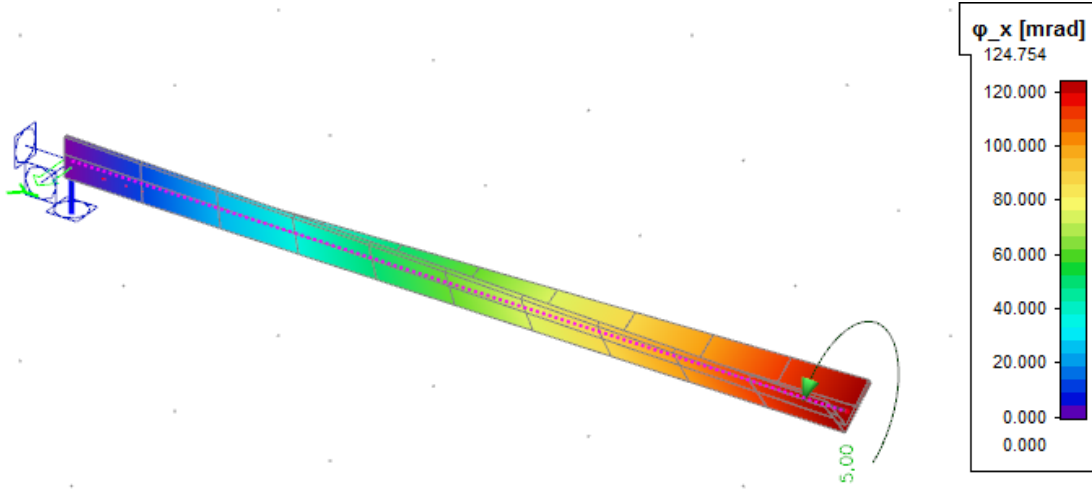


Figure 4.2: 3D-view of deformed L-shaped cantilever loaded in pure torsion

| ▲ | Name | dx [m] | Fibre | Case | σ_x [N/mm ²] | τ_{xy} / τ_{xs} [N/mm ²] | τ_{xz} / τ_{xs} [N/mm ²] |
|---|------|--------|---------|------|---------------------------------|--|--|
| 1 | B1 | 0,000 | Fibre14 | LC1 | 0,000 | -50,526 | 0,000 |
| 2 | B1 | 2,500- | Fibre14 | LC1 | 0,000 | -50,526 | 0,000 |
| 3 | B1 | 2,500+ | Fibre14 | LC1 | 0,000 | -50,526 | 0,000 |
| 4 | B1 | 5,000 | Fibre14 | LC1 | 0,000 | -50,526 | 0,000 |

Figure 4.3: Stress results for L-shaped cantilever loaded in pure torsion

| ▲ | Name | dx [m] | Case | u_x [mm] | u_y [mm] | u_z [mm] | φ_x [mrad] | φ_y [mrad] | φ_z [mrad] | U_{total} [mm] |
|---|------|--------|------|------------|------------|------------|--------------------|--------------------|--------------------|------------------|
| 1 | B1 | 0,000 | LC1 | 0,0 | 0,0 | 0,0 | 0,000 | 0,000 | 0,000 | 0,0 |
| 2 | B1 | 5,000 | LC1 | 0,0 | 0,0 | 0,0 | 124,754 | 0,000 | 0,000 | 0,0 |

Figure 4.4: Deformation results for L-shaped cantilever loaded in pure torsion

Now we can compare the results. Looking at table 4.1, we observe that the values from SCIA match the expected values very well.

Table 4.1: Comparison between theory and SCIA results for L-shaped cantilever

| | Theory | SCIA |
|--------------|--------------------------|--------------------------|
| τ_{max} | 50.526 N/mm ² | 50.526 N/mm ² |
| φ_x | 124.75 mrad | 124.75 mrad |

4.2 Double clamped beam

We will consider a beam that is clamped on both ends, similar to the example from the introduction. The cross section and the length of the beam are the same as in the previous example. Again the structure will be loaded with a torsional moment only, but we will consider three different positions for the load. The goal is to investigate whether the distribution of the torsional moment, and subsequently the shear stresses, are correct. The structure we will analyse is pictured in Figure 4.5.

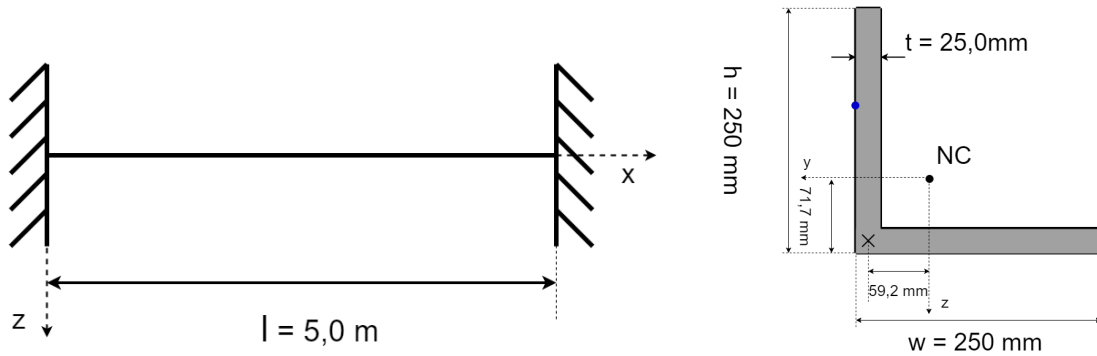


Figure 4.5: Double clamped cantilever beam with L-shaped cross-section

Expectation

We choose the loading positions the same as in the introduction, so at $1/2$, $1/4$ and $1/10$ of the span. These positions are pictured in Figure 4.6. Note that the dotted arrows indicate the position of the torsional moment, not to be confused with the location of a point load. The moment distribution due to these loading scenarios can be obtained by using the same solution strategy as in the introduction. There we found the torsional moment distribution of a double clamped structure is directly proportional to the position of the load. Applying equation (1.3) to this scenario three separate moment distribution graphs can be drawn. These can be found in Figure 4.7. With this moment distribution the shear stresses can be obtained by filling in equation (A.11).

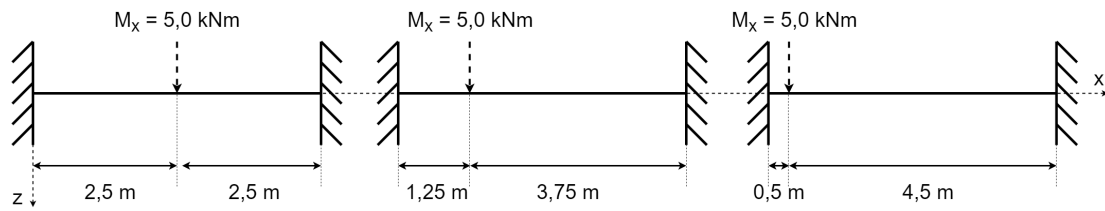


Figure 4.6: Loading positions double clamped cantilever

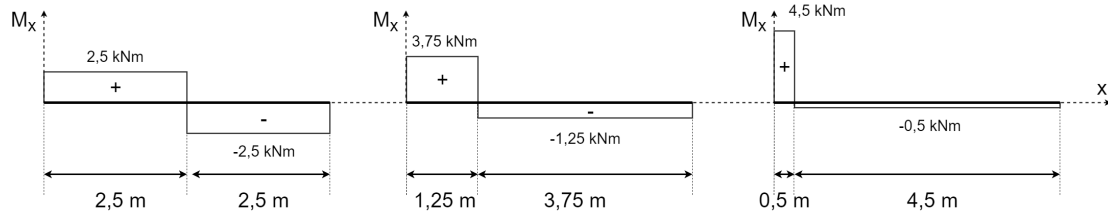


Figure 4.7: Expected moment distributions

Results in SCIA

The internal moment distribution given by SCIA matches our expectation. The results can be seen in Figure 4.8. The magnitude of the internal forces is correct, but the sign is different. Where we expected to see a positive value, SCIA reports a negative and vice-versa. This is due to the fact that SCIA can only display the values in the local coordinate system of the cross section, which is different than the coordinate system we have used in the calculation.

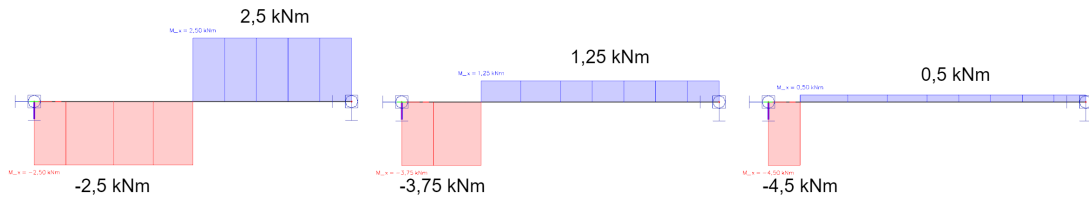


Figure 4.8: Internal moment distribution of double clamped beam in SCIA

The other check that needs to be done is whether this torsional moment leads to the correct shear stresses. Since the shear stresses are linear in M_x , they can be easily computed. The shear stress diagrams from SCIA can be found in Figure 4.9. A comparison between the expected shear stresses and the results from SCIA is made in table 4.2. Again the sign of the stresses is different than we would expect, but this can be attributed to the coordinate system choice. The magnitudes of the shear stresses do match our expectation.

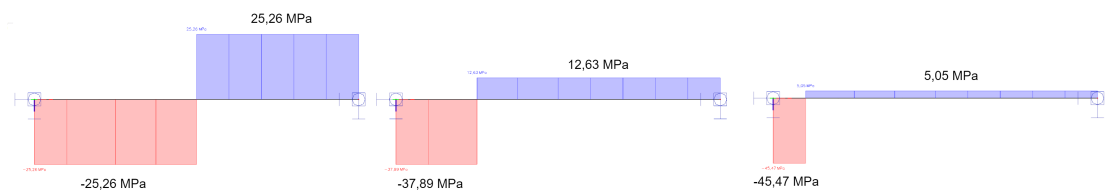


Figure 4.9: Shear stress results for double clamped beam in SCIA

Table 4.2: Shear stress comparison for double clamped beam

| | Expectation | | Shear stress in SCIA | |
|----------------|-------------------------|--------------------------|--------------------------|-------------------------|
| | part 1 | part 2 | part 1 | part 2 |
| Load midspan | 52.26 N/mm ² | -52.26 N/mm ² | -52.26 N/mm ² | 52.26 N/mm ² |
| Load 1/4 span | 37.89 N/mm ² | -12.63 N/mm ² | -37.89 N/mm ² | 12.63 N/mm ² |
| Load 1/10 span | 45.47 N/mm ² | -5.05 N/mm ² | -45.47 N/mm ² | 5.05 N/mm ² |

4.3 Findings

From the analysis of a single clamped cantilever beam, we have observed that the values of a calculation in SCIA match the expected values. Therefore we can say that the computation of torsional deformation and shear stresses for a basic torsion problem are correct. From the analysis of the double clamped beam in section 4.2, we have seen that the distribution of the internal torsional moment is correct in SCIA. This was determined using the shear stress distribution due to a torsional moment applied on different points on the span.

Chapter 5

Loading

The next step in the investigation is to consider the loading. Because there are no significant issues when considering geometry and boundary conditions, from now on the focus will be on different loading scenarios. Again we will consider a single clamped beam, which can be considered as a simple boundary condition. The same L-shaped cross section is chosen as in previous examples. We have already established in section 4.1 that for pure torsion, the results for this structure are in line with the theory. To investigate further, this chapter will discuss three different load cases:

- Pure bending with external torque
- Point load in normal force centre
- Point load in shear centre

5.1 Pure bending

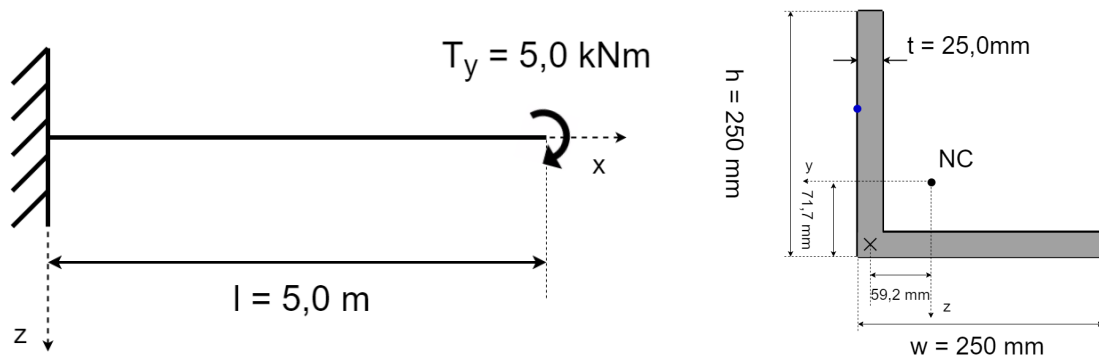


Figure 5.1: Cantilever beam with L-shaped cross-section

The structure is loaded with a moment T_y around the y -axis at the end of the span. Since this cross section is non-symmetrical, the moment of inertia I_{yz} is non-zero[3]. This means that in this example double bending will occur. For clarity reasons, only the main steps of the calculation will be shown in this section. For the complete calculation, reference is made to Appendix C.2 where a Maple file can be found. The constitutive relation for bending[3] is:

$$\begin{bmatrix} M_y \\ M_z \end{bmatrix} = \begin{bmatrix} EI_{yy} & EI_{yz} \\ EI_{yz} & EI_{zz} \end{bmatrix} \cdot \begin{bmatrix} \kappa_y \\ \kappa_z \end{bmatrix} \quad (5.1)$$

The cross-sectional properties have already been determined in section 3.2. These magnitudes can be found in table 3.2 and the Young's modulus for steel S235 in table 1.1. Also knowing

the moment distribution we obtain the following system:

$$\begin{bmatrix} 0 \\ 5.0 \cdot 10^6 \text{ Nmm} \end{bmatrix} = 10^{12} \cdot \begin{bmatrix} 14.8 \text{ Nmm}^2 & -8.7 \text{ Nmm}^2 \\ -8.7 \text{ Nmm}^2 & 14.8 \text{ Nmm}^2 \end{bmatrix} \cdot \begin{bmatrix} \kappa_y \\ \kappa_z \end{bmatrix} \quad (5.2)$$

Elaborating this we obtain the curvatures in y- and z-direction:

$$\begin{bmatrix} \kappa_y \\ \kappa_z \end{bmatrix} = \begin{bmatrix} 3.09 \cdot 10^{-7} \\ 5.21 \cdot 10^{-7} \end{bmatrix} \quad (5.3)$$

Now we can calculate the deflections using this curvature distribution. This is done using the theory from section 8.4 of Hartsuijker[1]. The result is:

$$\begin{bmatrix} u_y \\ u_z \end{bmatrix} = \begin{bmatrix} 3.859 \text{ mm} \\ 6.518 \text{ mm} \end{bmatrix} \quad (5.4)$$

The next step is to look at the results in SCIA. These results are presented in Figure 5.2 and 5.3. As expected, double bending occurs. The magnitudes of the deflection at the end of the cantilever are exactly the same as in equation (5.6). The sign of both deflections is opposite of what we have calculated. This is due to the fact that SCIA displays the deflections in the coordinate system of the cross section, which is different than the coordinate system used in the hand calculation.

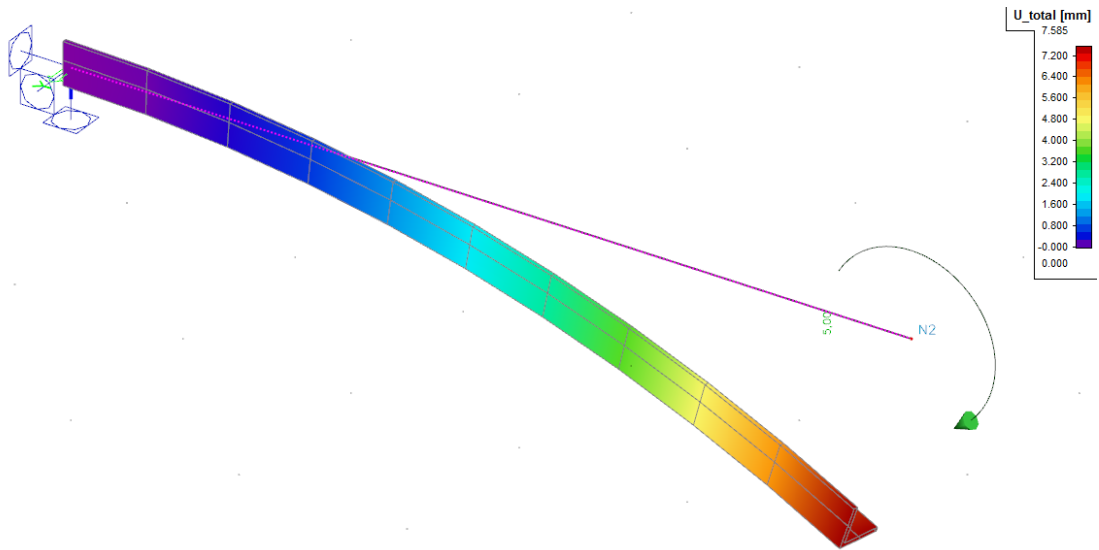


Figure 5.2: 3D-view of deflected L-shaped cantilever loaded in pure bending in SCIA

| ▲ | Name | dx [m] | Case | ux [mm] | uy [mm] | uz [mm] | φx [mrad] | φy [mrad] | φz [mrad] | Utotal [mm] |
|---|------|--------|------|--------------|---------------|---------------|------------|------------|-------------|--------------|
| 1 | B1 | 0,000 | LC1 | 0,000 | 0,000 | 0,000 | 0,0 | 0,0 | 0,0 | 0,000 |
| 2 | B1 | 5,000 | LC1 | 0,000 | -3,859 | -6,518 | 0,0 | 2,6 | -1,5 | 7,574 |

Figure 5.3: Table of deflections of L-shaped cantilever loaded in pure bending in SCIA

5.2 Point load in normal force centre

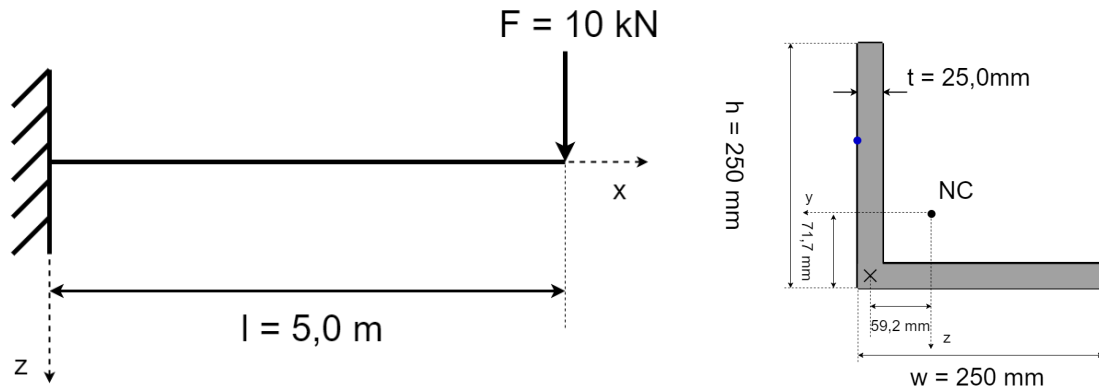


Figure 5.4: Cantilever beam loaded with a point load in the normal force centre

Table 5.1: Material Properties

| | Symbol | S235 |
|-----------------|--------|---------------------------------|
| Young's modulus | E | $210 \cdot 10^3 \text{ N/mm}^2$ |
| Shear modulus | G | $8.1 \cdot 10^4 \text{ N/mm}^2$ |

We will consider a cantilever with a L-shaped cross section, as shown in figure 5.4. The material used for this structure is described in table 5.1. The force F acts in the normal force centre. We know from the theory (section 5.5 of Hartsuijker[1]) that in L-shaped cross sections the normal force centre does not coincide with the shear force centre. Therefore the expectation is that in this case the force F will not only cause a load in Z -direction, but will also lead to a torsional moment. This torsional moment will cause shear stresses and a deformation around the x -axis. The calculation of the expected deformations is performed in two parts. First the deflection due to bending only is determined. Then the torsional deformation is calculated. Also the expected maximum shear stress and internal moment are calculated. The complete calculation procedure is presented in Appendix C.3, but for clarity reasons only the results are presented here. The expected deformations in y -, z - and x -direction are:

$$\begin{bmatrix} u_y \\ u_z \\ \varphi_x \end{bmatrix} = \begin{bmatrix} 25.73 \text{ mm} \\ 43.45 \text{ mm} \\ 14.77 \text{ mrad} \end{bmatrix} \quad (5.5)$$

The expected internal forces due to shear centre eccentricity are:

$$\begin{bmatrix} M_x \\ \tau_{max} \end{bmatrix} = \begin{bmatrix} 0.592 \cdot 10^6 \text{ Nmm} \\ 5.98 \text{ N/mm}^2 \end{bmatrix} \quad (5.6)$$

The results from SCIA are presented in Figures 5.5, 5.6, 5.7 and 5.8. The value for maximum shear stress was found with the option "consider torsion due to shear centre eccentricity" enabled. Turning this option off, the values in column " τ_{xy}/τ_{xs} " all reduced to zero.

Now we collect the expectations and the results from SCIA, to compare the magnitudes in table 5.2. From the 3D-overview and the deformation results, we observe no rotation around the x -axis. The deflection due to bending in y -direction is correct, but the value in z -direction shows some discrepancy. No torsional moment is reported. And finally, the maximum shear stress that SCIA reports is also different in value than our expectation.

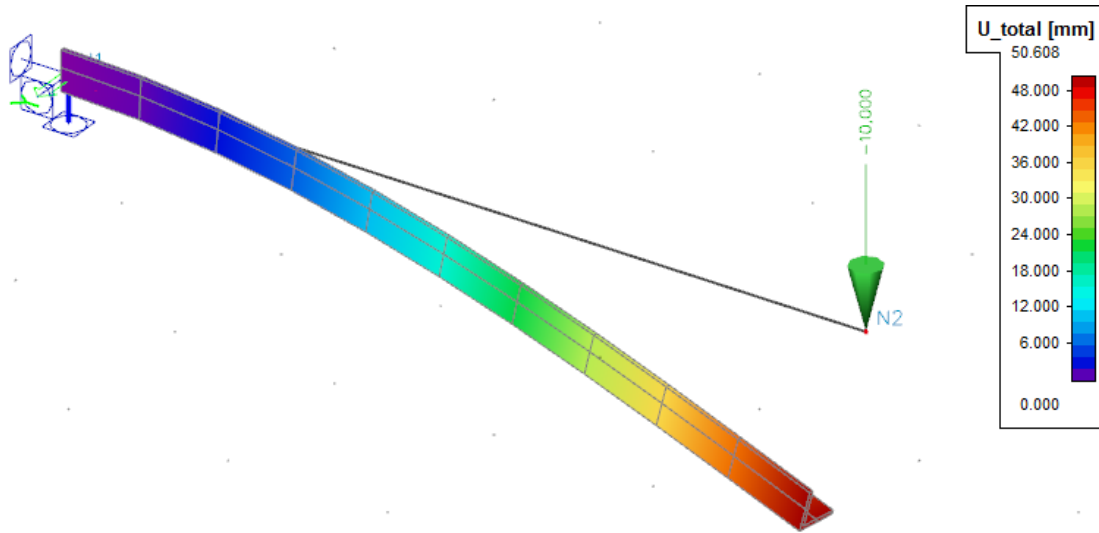


Figure 5.5: 3D-view of deformation of L-shaped Cantilever with load in NC

| ▲ | Name | dx [m] | Case | ux [mm] | uy [mm] | uz [mm] | φx [mrad] | φy [mrad] | φz [mrad] | Utotal [mm] |
|---|------|--------|-----------------------------|--------------|----------------|----------------|------------|-------------|-------------|---------------|
| 1 | B1 | 0,000 | Load in normal force centre | 0,000 | 0,000 | 0,000 | 0,0 | 0,0 | 0,0 | 0,000 |
| 2 | B1 | 2,500- | Load in normal force centre | 0,000 | -8,039 | -13,609 | 0,0 | 9,8 | -5,8 | 15,806 |
| 3 | B1 | 2,500+ | Load in normal force centre | 0,000 | -8,039 | -13,609 | 0,0 | 9,8 | -5,8 | 15,806 |
| 4 | B1 | 5,000 | Load in normal force centre | 0,000 | -25,726 | -43,512 | 0,0 | 13,0 | -7,7 | 50,548 |

Figure 5.6: Deformation result of L-shaped cantilever with load in NC

| ▲ | Name | dx [m] | Case | N [kN] | Vy [kN] | Vz [kN] | Mx [kNm] | My [kNm] | Mz [kNm] |
|---|------|--------|-----------------------------|--------------|--------------|---------------|--------------|----------------|--------------|
| 1 | B1 | 0,000 | Load in normal force centre | 0,000 | 0,000 | 10,000 | 0,000 | -50,000 | 0,000 |
| 2 | B1 | 2,500- | Load in normal force centre | 0,000 | 0,000 | 10,000 | 0,000 | -25,000 | 0,000 |
| 3 | B1 | 2,500+ | Load in normal force centre | 0,000 | 0,000 | 10,000 | 0,000 | -25,000 | 0,000 |
| 4 | B1 | 5,000 | Load in normal force centre | 0,000 | 0,000 | 10,000 | 0,000 | 0,000 | 0,000 |

Figure 5.7: Internal forces result of L-shaped cantilever with load in NC

| ▲ | Name | dx [m] | Fibre | Case | σx [MPa] | τxy / τxs [MPa] | τxz / τxs [MPa] |
|---|------|--------|---------|-----------------------------|----------|-----------------|-----------------|
| 1 | B1 | 0,000 | Fibre14 | Load in normal force centre | 32,029 | 8,485 | 1,244 |
| 2 | B1 | 2,500- | Fibre14 | Load in normal force centre | 16,015 | 8,485 | 1,244 |
| 3 | B1 | 2,500+ | Fibre14 | Load in normal force centre | 16,014 | 8,485 | 1,244 |
| 4 | B1 | 5,000 | Fibre14 | Load in normal force centre | 0,000 | 8,485 | 1,244 |

Figure 5.8: Stress result of L-shaped cantilever with load in NC

Table 5.2: Comparison between theory and SCIA for L-shaped cantilever with load in NC

| | Expectation | Result in SCIA |
|--------------|--------------------------|--------------------------|
| u_y | 25.73 mm | 25.73 mm |
| u_z | 43.45 mm | 43.51 mm |
| φ_x | 14.77 mrad | 0 |
| M_x | $0.592 \cdot 10^6$ Nmm | 0 |
| τ_{max} | 5.98 N/mm ² | 8.49 N/mm ² |

5.3 Point load in shear centre

The next loading scenario that will be addressed is a scenario where a point load is applied at the shear centre of the cross section. According to the theory, no torsion will occur. This means the structure will effect in y- and z-direction, but no axial deformation will be present. An schematic view of the structure is presented in Figure 5.9.

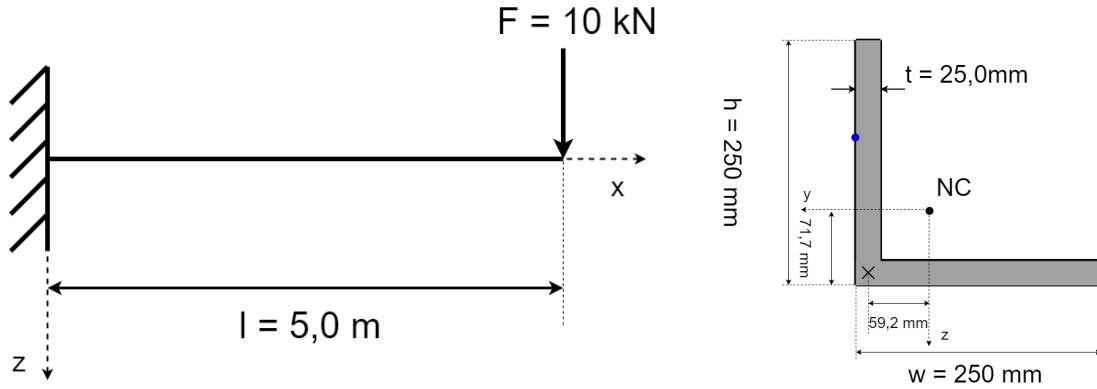


Figure 5.9: Cantilever beam loaded with a point load in the shear centre

The shear force centre is indicated with a cross in the drawing of the cross section. The location of this shear centre has already been determined. The eccentricity of this point with respect to the normal force centre is $d_y=59.21$ mm and $d_z=59.21$ mm. For the calculation process of this location, reference is made to Appendix C.1. Because the force has the same magnitude as in the previous example, and the dimensions of the structure have not changed, the deflections due to bending moments remain unchanged. The only difference is no rotation around the x-axis is to be expected. The expected deflections are:

$$\begin{bmatrix} u_y \\ u_z \end{bmatrix} = \begin{bmatrix} 25.73 \text{ mm} \\ 43.45 \text{ mm} \end{bmatrix} \quad (5.7)$$

In SCIA, the same structure is used as in the previous example. However, now the load is changed to a point load in the shear centre. Because there is no option to do this directly, the eccentricity of the load is inputted manually. The used offsets are $d_y=59.21$ mm and $d_z=59.21$ mm. The results from the calculation are presented in Figure 5.10, 5.11, 5.12 and 5.13.

All results are collected in table 5.3. The first observation from this table is that the magnitude of the deflection in y-direction is according to our expectation. The value for deflection in z-direction however, is not the same. But possibly the biggest discrepancy is that SCIA reports axial deformation around the x-axis. This is against our expectation. We also see an internal torsional moment in the results. The shear stresses that are reported due to “shear centre eccentricity”, again have a value of 8.49 N/mm².

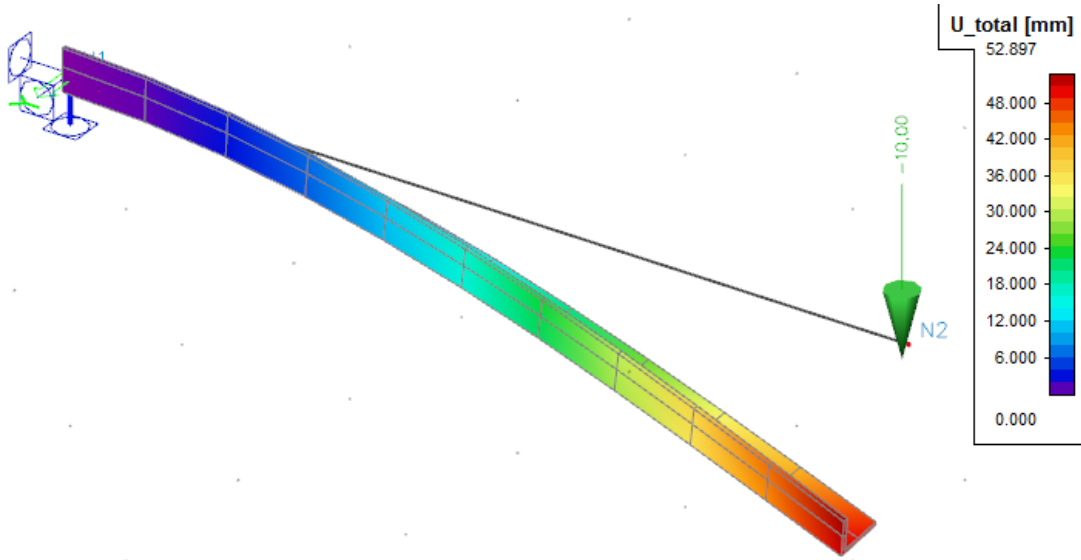


Figure 5.10: 3D-view of deflected L-shaped cantilever loaded in the shear centre in SCIA

| ▲ | Name | dx [m] | Case | ux [mm] | uy [mm] | uz [mm] | φx [mrad] | φy [mrad] | φz [mrad] | Utotal [mm] |
|---|------|--------|----------------------|--------------|----------------|----------------|-------------|-------------|-------------|---------------|
| 1 | B1 | 0,000 | Load in shear centre | 0,000 | 0,000 | 0,000 | 0,0 | 0,0 | 0,0 | 0,000 |
| 2 | B1 | 2,500- | Load in shear centre | 0,000 | -8,039 | -13,609 | 7,4 | 9,8 | -5,8 | 15,806 |
| 3 | B1 | 2,500+ | Load in shear centre | 0,000 | -8,039 | -13,609 | 7,4 | 9,8 | -5,8 | 15,806 |
| 4 | B1 | 5,000 | Load in shear centre | 0,000 | -25,726 | -43,512 | 14,8 | 13,0 | -7,7 | 50,548 |

Figure 5.11: Table of deflections of L-shaped cantilever loaded in the shear centre in SCIA

| ▲ | Name | dx [m] | Case | N [kN] | Vy [kN] | Vz [kN] | Mx [kNm] | My [kNm] | Mz [kNm] |
|---|------|--------|----------------------|--------------|--------------|---------------|---------------|----------------|--------------|
| 1 | B1 | 0,000 | Load in shear centre | 0,000 | 0,000 | 10,000 | -0,592 | -50,000 | 0,000 |
| 2 | B1 | 2,500- | Load in shear centre | 0,000 | 0,000 | 10,000 | -0,592 | -25,000 | 0,000 |
| 3 | B1 | 2,500+ | Load in shear centre | 0,000 | 0,000 | 10,000 | -0,592 | -25,000 | 0,000 |
| 4 | B1 | 5,000 | Load in shear centre | 0,000 | 0,000 | 10,000 | -0,592 | 0,000 | 0,000 |

Figure 5.12: Internal forces results from SCIA

| ▲ | Name | dx [m] | Fibre | Case | σx [MPa] | τxy / τxs [MPa] | τxz / τxs [MPa] |
|---|------|--------|---------|----------------------|----------|-----------------|-----------------|
| 1 | B1 | 0,000 | Fibre14 | Load in shear centre | 32,029 | 2,502 | 1,244 |
| 2 | B1 | 2,500- | Fibre14 | Load in shear centre | 16,015 | 2,502 | 1,244 |
| 3 | B1 | 2,500+ | Fibre14 | Load in shear centre | 16,014 | 2,502 | 1,244 |
| 4 | B1 | 5,000 | Fibre14 | Load in shear centre | 0,000 | 2,502 | 1,244 |

Figure 5.13: Stress results with option 'consider torsion due to shear centre eccentricity' enabled

| ▲ | Name | dx [m] | Fibre | Case | σx [MPa] | τxy / τxs [MPa] | τxz / τxs [MPa] |
|---|------|--------|---------|----------------------|----------|-----------------|-----------------|
| 1 | B1 | 0,000 | Fibre14 | Load in shear centre | 32,029 | -5,983 | 1,244 |
| 2 | B1 | 2,500- | Fibre14 | Load in shear centre | 16,015 | -5,983 | 1,244 |
| 3 | B1 | 2,500+ | Fibre14 | Load in shear centre | 16,014 | -5,983 | 1,244 |
| 4 | B1 | 5,000 | Fibre14 | Load in shear centre | 0,000 | -5,983 | 1,244 |

Figure 5.14: Stress results with option 'consider torsion due to shear centre eccentricity' not enabled

Table 5.3: Comparison between theory and SCIA for L-shaped cantilever with load in shear centre

| | Expectation | Result in SCIA |
|--------------|-------------|------------------------|
| u_y | 25.73 mm | 25.73 mm |
| u_z | 43.45 mm | 43.51 mm |
| φ_x | 0 mrad | 14.8 |
| M_x | 0 | $0.592 \cdot 10^6$ Nmm |
| τ_{max} | 0 | 8.49 N/mm ² |

5.4 Findings

The analysis of different load scenarios has led to some unexpected results. Although the calculations for pure torsion(section 4.1), and pure bending(section 5.1) both are in line with the theory, it seems the inconsistencies start when bending and torsion are combined. In section 5.2 we observe that no torsional deformation and internal torsional moment are calculated. We also observe shear stresses that have a different magnitude than we would expect. Although the reported stresses are bigger than expected and thus do not cause an unsafe situation, it raises questions on SCIA's solution strategy.

Chapter 6

Conclusion

Recalling from the introduction chapter, several questions were raised regarding a torsion calculation in SCIA Engineer. Following from a suspicion that was present regarding torsion calculations for non-symmetrical cross sections, a structure was considered where shear centre eccentricity played a significant role in the stress calculations. The magnitudes of the shear stresses found in a double clamped structure loaded in bending and torsion were 60% lower than the stresses that were expected by using a theoretical approach. In engineering practices this discrepancy can lead to very unsafe situations, so the issue should be addressed. This led to an investigation on different aspects of the torsion calculation, with the ultimate goal to formulate an advice for the software developers. To accomplish this, the area of interest has to be narrowed down. The investigation described in this paper consists of three sections. First the geometry was checked, then the boundary conditions were considered and lastly different loading situations were applied. Below, for each of these sections the results are presented and conclusions are drawn.

6.1 Geometry

The first check performed in this paper was whether the determination of cross sectional properties was performed correctly in SCIA. This research was performed in Chapter 3. The question formulated in the introduction was:

- Does SCIA calculate cross sectional properties in the correct way?

Two types of cross section were investigated, starting with a symmetrical I-shaped section. This type of cross section is very common in engineering applications, thus very interesting to consider first. The fact that this cross section is symmetrical in two axes, means the shear force centre coincides with the normal force center. This left mostly the values for part I of SCIA's geometry calculation, the values for bi-axial bending and axial force, to be checked. A comparison between the values from a hand calculation and the values from SCIA was made, but yielded no discrepancies.

Secondly, an L-shaped cross section was considered. In theory, this type of cross section is symmetrical in only one axis. This means the position of the shear centre does not coincide with the normal force centre. This fact made this cross section very interesting to investigate, because forces applied in the normal force centre will cause torsion to occur. When the values obtained by a hand calculation were compared to the values from SCIA, most magnitudes matched. Only the determination of the position of the shear centre yielded different results, as presented in table 6.1:

A discrepancy in the calculation of the shear centre was observed between the theory and SCIA. The difference between the expectation and the observed value was 0.2 mm. However, since this

| | Expectation | SCIA | Difference |
|---|-------------|----------|------------|
| Eccentricity of shear centre in principle y-direction | 83.74 mm | 83.97 mm | 0.23 mm |

Table 6.1: Comparison between expectation and SCIA

difference is very small, it is not likely to be the cause of the issue described in the introduction. Therefore the choice was made not to investigate this any further.

6.2 Boundary Conditions

The next question that was raised regarded the boundary conditions. This question was:

- Do different boundary conditions influence the torsion results in SCIA?

The checks to formulate an answer to this question were performed in Chapter 4. Here two different boundary conditions were considered for a beam with an L-shaped cross section. First a single clamped cantilever beam was analysed. A simple torsional loading scenario was chosen, and the results from a hand calculation were compared to a calculation in SCIA. This test was performed to determine whether for a basic torsional problem, the shear stresses and torsional deformation is computed according to our expectation. The results from a calculation in SCIA matched the expected values, so this confirmed there are no issues with the calculation of torsional deformation and shear stresses for a basic torsional problem.

Now a double clamped beam is considered. This check determines whether the distribution of the internal torsional moment over the beam is correct. Again a non-symmetrical L-shaped cross section was chosen. The structure was analysed for three different positions of the load, similar to the example from the introduction. However, now the load was chosen as a pure torsional moment. The results from a calculation in SCIA showed no discrepancies compared to the expected values. Therefore we can state that no issues are present in the distribution of internal torsional moments.

For both the single-clamped situation and the double-clamped situation, the calculation in SCIA was correct. Therefore it can be concluded that the boundary conditions have no influence on the results of torsion calculations in SCIA.

6.3 Loading

The third question that was formulated in the introduction was meant to investigate the influence of different loading situations on the results for torsion calculations in SCIA. The question was:

- Is the discrepancy between the theory and SCIA influenced by varying the loading?

In Chapter 5, three different loading scenarios were considered for the same structure. The structure consisted of a single-clamped L-shaped cantilever. The first check that was performed was if the deflections of a non-symmetrical cross section loaded in bending only were considered, the values of a hand calculation matched the results from SCIA. The structure was analysed with a hand calculation first. Comparing the results from this calculation to the results from SCIA, no differences were found. This means SCIA does use the correct solution strategy for non-symmetrical cross sections loaded in bending.

The second load scenario that was applied consisted of a point load in the normal force centre. It was previously established that this loading type should cause torsional deformation of the beam, due to shear centre eccentricity of the cross section. However, observing the results obtained from SCIA, no torsional deformation was reported. Also no internal moment around the

x-axis was seen, although this was expected. When the results for shear stresses were checked, another inconsistency was found. The shear stress did not have the expected magnitude. Although an option is present in the program to “consider torsion due to shear centre eccentricity”, incorrect shear stresses were found. The stresses reported with this option enabled were higher than expected.

The final loading scenario that was considered, was similar to the previous scenario. However, the point of application of the force was now moved to the shear centre. According to the theory, this loading situation would cause pure bending of the structure. However, in this case SCIA does report torsional deformation. Also an internal moment around the x-axis, and shear stresses due to torsion were reported. The difference between the shear stresses with the option “consider torsion due to shear centre eccentricity” enabled and disabled was the same exact value as in the load case where the load was applied in the normal force centre.

Combining the knowledge gathered from these three checks, some conclusions can be drawn about the influence of loading situation on torsion results. The first is that for a beam loaded in pure bending or pure torsion, the values in SCIA match the expectation. However, when a load case is considered where torsion due to shear centre eccentricity is present, the results for the torsional deformation are not correct. In these cases also the internal torsional moment is not reported correctly. The option “consider torsion due to shear centre eccentricity” displays shear stresses in non-symmetrical cross sections loaded in the normal force centre. However, the magnitude of these stresses is not correct.

Chapter 7

Recommendations

Stiffness Matrix

It has been established in this report that the problems regarding torsion in SCIA engineer only occur when shear centre eccentricity is present. Calculations on pure bending and pure torsion produce correct results when compared to the theory. Only when a load is applied in the normal force centre of a non-symmetrical cross section, no torsional deformation and internal torsional moment in the structure are reported. This is not in line with the theory. Given these symptoms, an issue may be present in the calculation of beam element stiffness for the stiffness matrix. If shear centre eccentricity in this matrix is not implemented correctly or even missing completely, this may explain the unexpected results. Perhaps the solution is very simple, and the problem can be eliminated by adding the shear centre eccentricity to the offset that an element normal centre line may have with respect to the line drawn in the model.

Shear stresses

The results from the research in this paper indicate that SCIA calculates the shear stresses in post-processing, which is after the output file from the kernel is imported into the Graphical User Interface. In the 3D-stress results section, SCIA gives the option “consider torsion due to shear centre eccentricity”. With this option enabled, shear stress results are displayed. However, the magnitude of these shear stresses differ from their theoretical expectation. This issue was presented in the introduction of this report, in section 1.2. When the stiffness matrix is corrected, the shear stresses due to torsion will be computed directly from the internal torsional moments. This means the value will be correct, independent of shear centre eccentricity. Therefore this option and the underlying code can be removed.

Bibliography

- [1] Coenraad Hartsuijker, *Toegepaste Mechanica - deel 2: spanningen, vervormingen, verplaatsingen*, Academic Service, Schoonhoven, 2nd edition, 2003.
- [2] Hans Welleman, *Introduction into Continuum Mechanics*, TU Delft, December 2007
- [3] Hans Welleman, *Lecture notes for Structural Mechanics 4 - Module: Non-symmetrical and inhomogeneous cross sections*, TU Delft, April 2017

Appendices

Appendix A

Torsion Theory

In this paper, structures will be discussed where torsion plays a role. To provide some background on the theory of torsion, this paragraph is presented to provide the reader with the necessary explanation of the used formulas.

Coordinate system

First a coordinate system is defined. We will use the coordinate system pictured in Figure A.1. We observe a xyz -coordinate system where the x -axis coincides with the fibres in the normal

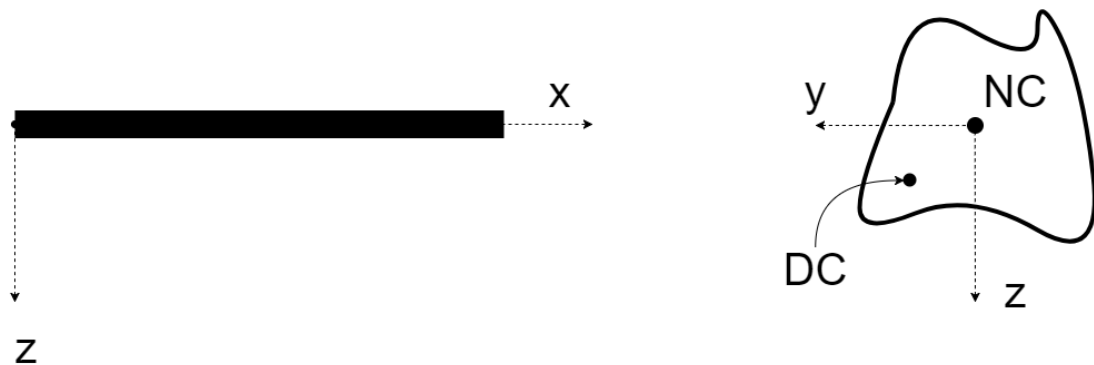


Figure A.1: Definition of coordinate Axes

force centre of the beam. This normal force centre, denoted by NC, is defined as “The point in a cross section where the resultant normal force, caused by extension of the element, acts” [1, Chapter 3.1.3, p.69]. This also means it is the point of the cross section where, if a normal force is applied, no bending moments will occur in the element. Also a shear force centre can be defined. According to (Hartsuijker, 2003) [Chapter 5.5, p.331]: “If the line of action of the shear force goes through the point that is called the shear force centre DC, no torsion will occur”. This point is denoted by DC in Figure A.1. In symmetrical cross sections, the shear force center coincides with the normal force centre. The z -axis is pointed downwards, so positive loads will cause deformations in downward direction. Also rotations have to be described. A rotation φ_x around the x -axis is defined as a rotation from y to z . A φ_y is defined as a rotation from z to x and a rotation φ_z from x to y . A positive rotation is caused by a positive moment. The signs of the stresses also follow these directions.

Loading types

To introduce the concept of torsion, we start with two simple loading types in 2D. In Figure



Figure A.2: 2D-loading types

A.2, two different loading situations are sketched. In the first case, the structure is loaded with a normal force. This will cause deformation of the element, in this case extension. The second example is loaded in bending. The loading causes bending moments to occur, which lead to the structure deforming in a curved shape. For some engineering purposes it will suffice to only consider these loading types for stress and strain calculations. If we expand to 3D however, another loading type arises which needs to be addressed. This loading type is torsion, and is visualised in Figure A.3. Torsion occurs when an element is loaded with a moment around the beam axis. This type of loading causes axial deformation, which leads to a rotation of the cross section.

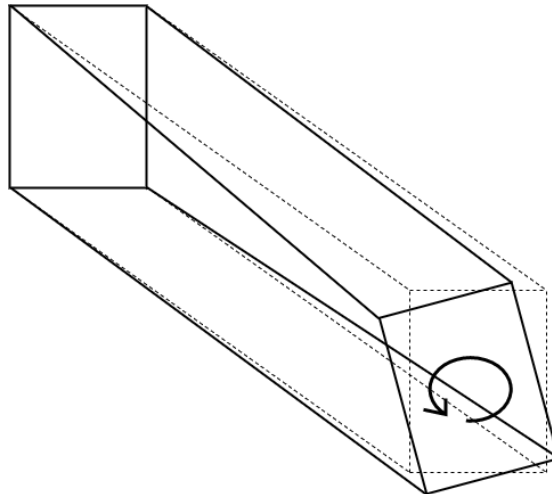


Figure A.3: Torsion in a beam element

Stress and strain caused by torsion

To analyse stresses and strains caused by torsion, in this paragraph three types of cross sections are presented. The first type of cross section that will be discussed is the thin walled circular cross section. The second type is a closed circular cross section. The third type that will be discussed is a thin walled open cross section. For these three types, the formulas will be presented for the calculation of torsional deformation and shear stresses. The theory presented here will be used throughout the paper, which means this section is meant as a reference. The theory that is used is extracted from the book on engineering mechanics by Coenraad Hartsuijker[1]. For derivations and more information a reference is made to this book. Here only the results of these derivations are presented, since proving the formulas is beyond the scope of this paper.

Thin walled circular cross section

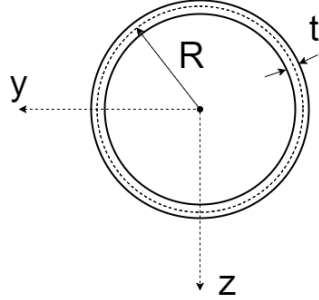


Figure A.4: Example of thin walled circular cross section

In Figure A.4 an example of a thin walled circular cross section is shown. As presented in (Hartsuijker, 2003)[1] in chapter 6.2 on page 373, the shear stresses for thin walled circular cross sections can be assumed constant over the thickness of the material. The value of this stress can be computed by equation (A.1).

$$\tau = \frac{M_t \cdot R}{I_p} \quad (\text{A.1})$$

Here, M_t is the torsional moment present in the cross section, R is the radius of the circle and I_p is the polar moment of inertia. This moment of inertia has a value of

$$I_p = 2\pi R^3 t \quad (\text{A.2})$$

Where R is the radius of the circle and t is the thickness of the material. Subsequently, a cross section loaded in torsion will undergo torsional deformation. This deformation is defined as a rotation around the x -axis, denoted by φ_x . The constitutive relation between torsional moment and deformation is given by

$$\chi = \frac{d\varphi_x}{dx} = \frac{M_t}{GI_p} \quad (\text{A.3})$$

Where G is the material specific torsion constant, and χ is the contortion of the beam. This contortion value shows large similarities to the ε in case of extension and κ in case of bending. For constant torsional moment, the rotation due to this moment can be computed by

$$\varphi_x = \frac{M_t \cdot l}{GI_p} \quad (\text{A.4})$$

Where l is the length of the element.

Closed circular cross section

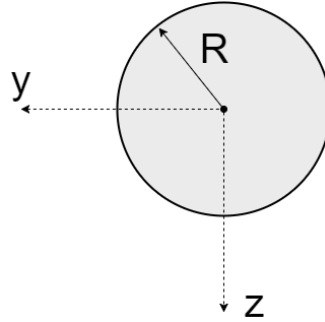


Figure A.5: Example of closed circular cross section

The next step is to expand to a closed circular cross section. An example of this type of cross section is presented in figure A.5. This type of cross section is thought to be built up out of multiple thin-walled sections fitted together. The constitutive relation from equation (A.3) still holds, but the polar moment of inertia now has a different value, given by (A.5).

$$I_p = \frac{1}{2}\pi R^4 \quad (\text{A.5})$$

The assumption of constant stress over the thickness is not valid anymore for this case. Now we observe a shear stress that is linear in the radius of the circle. This shear stress has a value of:

$$\tau(r) = \frac{M_t \cdot r}{I_p} \quad (\text{A.6})$$

Where r is the distance to the centre line of the circle.

Thin walled open cross sections

An example of a thin walled open cross section is presented in figure A.6. It can be proven that

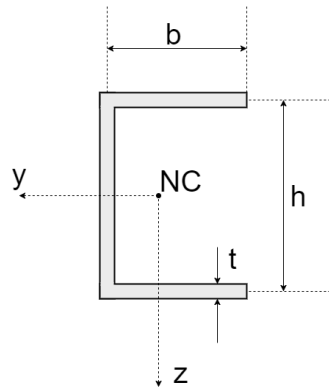


Figure A.6: Example of thin walled open cross section

for thin walled open cross sections, the constitutive relation for torsion deformation is of the form:

$$\varphi_x = \frac{M_t \cdot l}{GI_t} \quad (\text{A.7})$$

where I_t is now the torsional moment of inertia. This is a different value than the polar moment of inertia we used before, and can be computed by:

$$I_t = \sum_{i=1}^n \frac{1}{3} h_i t_i^3 \quad (\text{A.8})$$

Which is the summation of the torsional moments of inertia of every strip element out of which the cross section is built up. For each of these strip elements, h is the height and t is the thickness of the element. For the cross section of the example in Figure A.6, this leads to a torsional moment of inertia of

$$I_t = \frac{1}{3}ht^3 + \frac{2}{3}bt^3 \quad (\text{A.9})$$

For thin walled open cross sections, the shear stresses are proportional to the distance to the centre line of the elements. The formula to calculate the stresses is:

$$\tau = \frac{M_t \cdot s_c}{\frac{1}{2}I_t} \quad (\text{A.10})$$

Where s_c is the distance to the centre line of the element. For stress calculations, we are mostly interested in the maximum shear stress. From this theory, we now know the maximum shear stress occurs when $s_c = \frac{t}{2}$. With this knowledge we can write an expression for the maximum shear stress:

$$\tau_{max} = \frac{M_t \cdot t}{I_t} \quad (\text{A.11})$$

Appendix B

Framework Analysis

For the automated calculation and analysis of structures a lot of different software is available on the market. The SCIA Engineer software package that is being used throughout this paper is a 'Framework Analysis' program. It also incorporates finite element technology. To understand how the program works, it is important to look at all the individual steps the software takes to get from an inputted structure to a complete structural analysis. To illustrate how this is done, in this chapter an overview will be presented of the key steps to get from input to a calculation, and ultimately to a usable result. Because this would get very complicated very fast if we would discuss every single aspect of the process, we will use a simplification of reality. Although this means we will not discuss some processes in the program, it will illustrate the operation of the software in a clean and simple manner.

B.1 Overview

A flowchart of the steps necessary to get to a calculation is pictured in Figure B.1. The process can be roughly divided into three steps. The first step is the generation of an input file for the kernel. In this file, for each element in the framework, a stiffness matrix is generated. Also the material properties are imported from the GUI and the loads are processed. The second step is the actual calculation. This is done in the 'kernel', which is the mathematical heart of the software. Here a large K-matrix is generated, in which the stiffness matrices for all the individual frame elements are assembled. This leads to a large system of equations, that can be solved for all the deflections. These deflections are then substituted back into the individual stiffness relations, to obtain the internal forces. The third and last step, is importing these values in the output file back into the graphical user interface. During this final step the unity checks are performed and also the stresses in the cross sections can be computed. Each of the steps will be further elaborated in the following paragraphs.

B.2 Generation of input file

The first step in any frame analysis software is the generation of the input file. The structure that has been created by the user has to be converted into a model that can be evaluated. This means the structure in the graphical interface first has to be divided into individual elements. To illustrate how this is done, we will consider a simple portal structure as pictured in Figure B.2. The elements have a rigid connection in node B and C. The structure is loaded with a unit moment 'T' in node B. The two supports in A and D are hinges, and a third support in C is added to prevent swaying of the structure. This means all the nodes can only rotate, no lateral displacements are possible. To start the modelling of this structure, we first divide the structure into three individual, static determinate beams. The model becomes Figure B.3. Then we consider the beam between A and B. We are looking for a system of equations in the

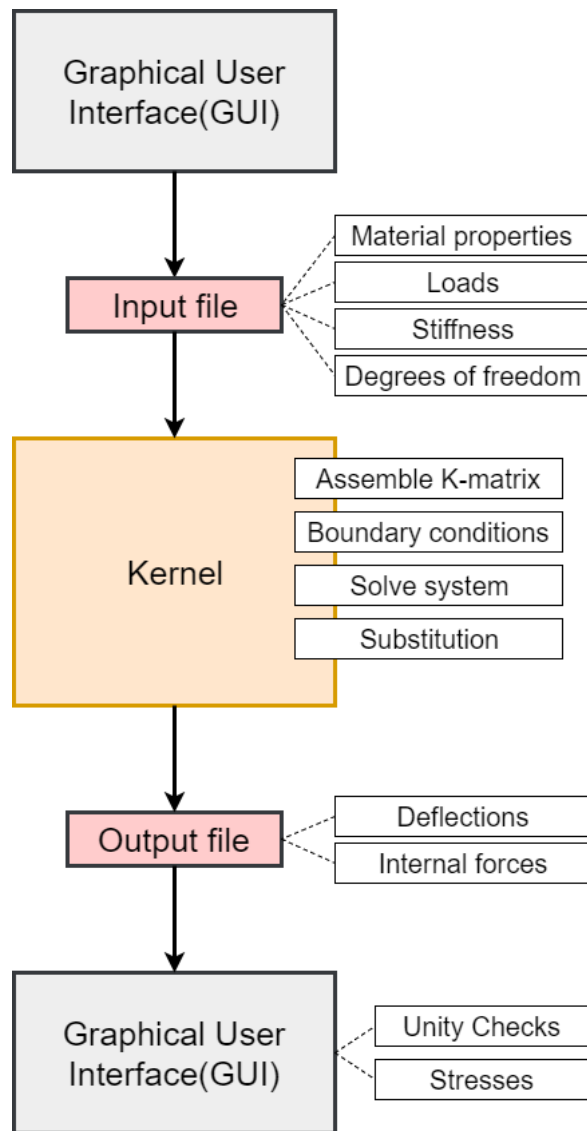


Figure B.1: Schematic overview of framework software

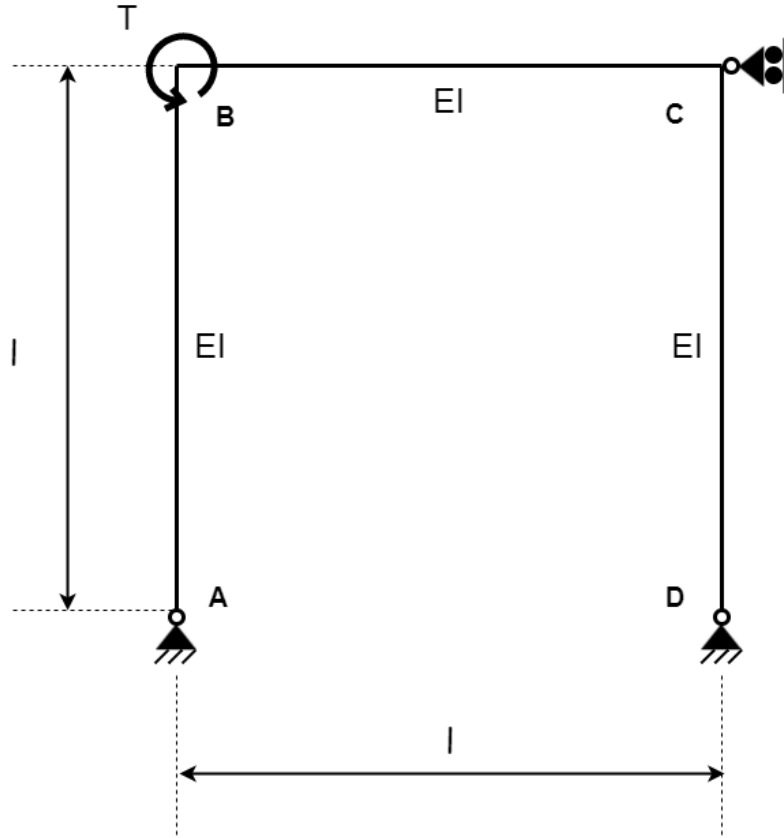


Figure B.2: Portal Structure

form:

$$\mathbf{m} = \bar{K} \cdot \boldsymbol{\varphi} \rightarrow \begin{bmatrix} M_A \\ M_B \end{bmatrix} = \begin{bmatrix} k_{aa} & k_{ab} \\ k_{ba} & k_{bb} \end{bmatrix} \cdot \begin{bmatrix} \varphi_A \\ \varphi_B \end{bmatrix} \quad (\text{B.1})$$

Where \mathbf{m} is the load vector, $\boldsymbol{\varphi}$ is the displacement vector and \bar{K} is the flexibility matrix. In words this equation means we have to find relations between the moments in the nodes and the rotations of the elements connected to the nodes. These can be found by solving the fourth order differential equation for bending. The solution for this simple load case is already known and can be found in the 'forget-me-nots'. To simplify things, we will first set φ_A to 0, while setting φ_B to 1. This leaves us with two equations.

$$\begin{bmatrix} M_A \\ M_B \end{bmatrix} = \begin{bmatrix} k_{aa} & k_{ab} \\ k_{ba} & k_{bb} \end{bmatrix} \cdot \begin{bmatrix} 0 \\ 1 \end{bmatrix} \rightarrow \begin{bmatrix} M_A \\ M_B \end{bmatrix} = \begin{bmatrix} k_{ab} \\ k_{bb} \end{bmatrix} \quad (\text{B.2})$$

This means if we find the moments in A and B due to a unit rotation in B, we obtain the values of k_{ab} and k_{bb} . The rotation in B due to a moment in B can be found in Figure B.4. However, we are interested in the moment due to a rotation. This relation can be obtained by rewriting the expression, knowing that φ_B has a value of 1:

$$\varphi_B = \frac{M_B \cdot l}{4EI} = 1 \rightarrow M_B = \frac{4EI}{l} \rightarrow k_{bb} = \frac{4EI}{l} \quad (\text{B.3})$$

We also know from the 'forget-me-nots', that in this type of loading situation the moment in the support in A will be half the moment excited at B. This means:

$$M_A = \frac{M_B}{2} = \frac{2EI}{l} \rightarrow k_{ab} = \frac{2EI}{l} \quad (\text{B.4})$$

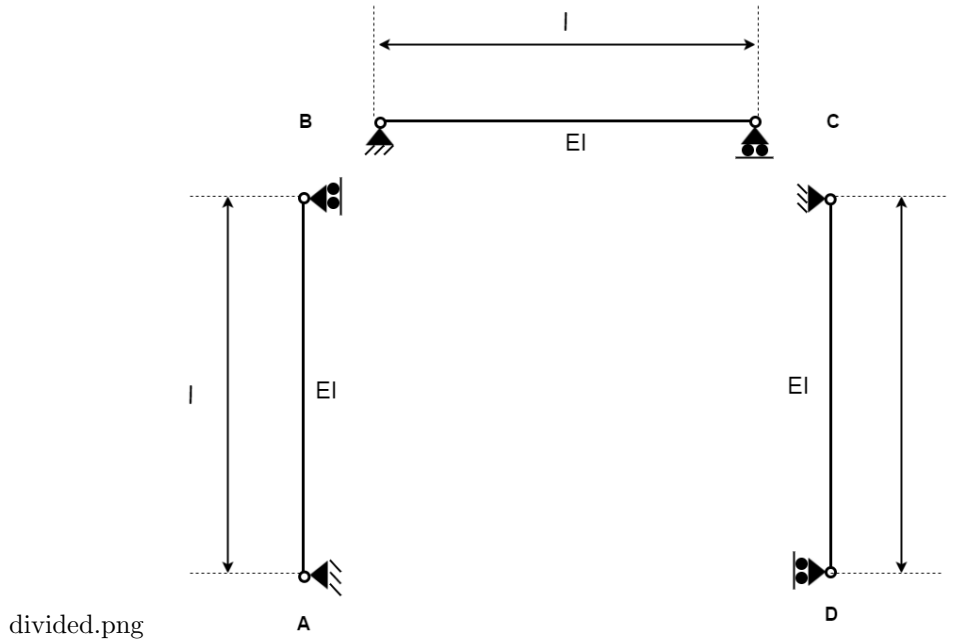


Figure B.3: Portal Structure divided into individual elements

Filling in the values for k_{ab} and k_{bb} , we obtain the system:

$$\begin{bmatrix} M_A \\ M_B \end{bmatrix} = \begin{bmatrix} k_{aa} & \frac{2EI}{l} \\ k_{ba} & \frac{4EI}{l} \end{bmatrix} \cdot \begin{bmatrix} \varphi_A \\ \varphi_B \end{bmatrix} \quad (\text{B.5})$$

Now we set the value of φ_A to 1 and the value of φ_B to 0. In a similar manner, we obtain the values for k_{aa} and k_{ba} . The final system of equations for the first element becomes:

$$\begin{bmatrix} M_A \\ M_B \end{bmatrix} = \begin{bmatrix} \frac{4EI}{l} & \frac{2EI}{l} \\ \frac{2EI}{l} & \frac{4EI}{l} \end{bmatrix} \cdot \begin{bmatrix} \varphi_A \\ \varphi_B \end{bmatrix} \quad (\text{B.6})$$

The process described above is repeated for all three elements in the framework. This leads to three individual flexibility relations; one for each element. In this case the flexibility matrices are identical, because the lengths and stiffnesses of all the elements are the same. The relations are:

$$\begin{aligned} \begin{bmatrix} M_A \\ M_B \end{bmatrix} &= \begin{bmatrix} \frac{4EI}{l} & \frac{2EI}{l} \\ \frac{2EI}{l} & \frac{4EI}{l} \end{bmatrix} \cdot \begin{bmatrix} \varphi_A \\ \varphi_B \end{bmatrix} \\ \begin{bmatrix} M_B \\ M_C \end{bmatrix} &= \begin{bmatrix} \frac{4EI}{l} & \frac{2EI}{l} \\ \frac{2EI}{l} & \frac{4EI}{l} \end{bmatrix} \cdot \begin{bmatrix} \varphi_B \\ \varphi_C \end{bmatrix} \\ \begin{bmatrix} M_C \\ M_D \end{bmatrix} &= \begin{bmatrix} \frac{4EI}{l} & \frac{2EI}{l} \\ \frac{2EI}{l} & \frac{4EI}{l} \end{bmatrix} \cdot \begin{bmatrix} \varphi_C \\ \varphi_D \end{bmatrix} \end{aligned} \quad (\text{B.7})$$

In SCIA, this is the end of the first step. Loads, stiffness and length of all the elements are written to an input file for the kernel. In reality, a lot more data is reported than we have demonstrated above. For example distributed loads are taken into account and torsion stiffness and deformation is added. Also the model in SCIA is 3D, whereas our model only has two dimensions. All these features are implemented in the input file, but the overall process is the same as we have done.

B.3 The Kernel

The previous paragraph has presented how a mathematical model is generated for a framework structure. Now the input file has been generated, the actual calculation can be made. This is

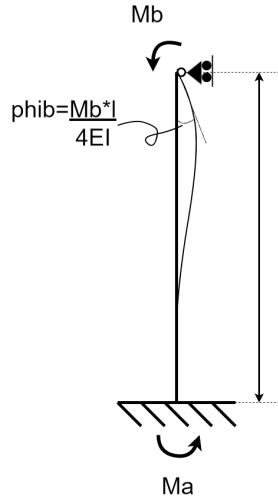


Figure B.4: Individual element

done in the kernel. The first step in the kernel is to assemble the individual flexibility relations in one large system of equations. In our case we have four nodes where a torque can be applied, and four following unknown rotations. This means we will have to generate a system of four equations and four unknowns, as shown below:

$$\begin{bmatrix} T_A \\ T_B \\ T_C \\ T_D \end{bmatrix} = \begin{bmatrix} k_{aa} & k_{ab} & k_{ac} & k_{ad} \\ k_{ba} & k_{bb} & k_{bc} & k_{bd} \\ k_{ca} & k_{cb} & k_{cc} & k_{cd} \\ k_{da} & k_{db} & k_{dc} & k_{dd} \end{bmatrix} \cdot \begin{bmatrix} \varphi_A \\ \varphi_B \\ \varphi_C \\ \varphi_D \end{bmatrix} \quad (\text{B.8})$$

In the scenario from Figure B.2 only a unit torque at node B is applied. Substituting this and assembling all the individual flexibility relations from equation (B.7) by adding them to the 4x4 matrix, we obtain:

$$\begin{bmatrix} 0 \\ 1 \\ 0 \\ 0 \end{bmatrix} = \begin{bmatrix} \frac{4EI}{l} & \frac{2EI}{l} & 0 & 0 \\ \frac{2EI}{l} & \frac{8EI}{l} & \frac{2EI}{l} & 0 \\ 0 & \frac{2EI}{l} & \frac{8EI}{l} & \frac{2EI}{l} \\ 0 & 0 & \frac{2EI}{l} & \frac{4EI}{l} \end{bmatrix} \cdot \begin{bmatrix} \varphi_A \\ \varphi_B \\ \varphi_C \\ \varphi_D \end{bmatrix} \quad (\text{B.9})$$

This system of equations can be described by $\mathbf{T} = \overline{\mathbf{K}} \cdot \boldsymbol{\varphi}$. Now we want to find the rotation vector $\boldsymbol{\varphi}$, while load vector \mathbf{T} and flexibility matrix $\overline{\mathbf{K}}$ are known. From linear algebra we know:

$$\mathbf{T} = \overline{\mathbf{K}} \cdot \boldsymbol{\varphi} \rightarrow \boldsymbol{\varphi} = \overline{\mathbf{K}}^{-1} \cdot \mathbf{T} \quad (\text{B.10})$$

Where $\overline{\mathbf{K}}^{-1}$ is the inverse of the flexibility matrix. Finding the inverse of a 4x4 matrix by hand would lead to a very long calculation, so this is left to Maple. This Maple file can be found in Appendix [reference]. The solution becomes:

$$\overline{\mathbf{K}}^{-1} \cdot \mathbf{T} = \begin{bmatrix} \varphi_A \\ \varphi_B \\ \varphi_C \\ \varphi_D \end{bmatrix} = \frac{l}{EI} \cdot \begin{bmatrix} -\frac{7}{90} \\ \frac{7}{45} \\ -\frac{2}{45} \\ \frac{1}{45} \end{bmatrix} \quad (\text{B.11})$$

Now we have obtained the rotations for all the nodes of the structure. However, the internal forces are still unknown. These can be found by substituting the now known rotations back into

the individual flexibility relations of the elements. This is done below:

$$\begin{aligned}
 \begin{bmatrix} M_A \\ M_B \end{bmatrix} &= \begin{bmatrix} \frac{4EI}{2EI} & \frac{2EI}{4EI} \\ \frac{l}{l} & \frac{l}{l} \end{bmatrix} \cdot \begin{bmatrix} -\frac{7 \cdot l}{90EI} \\ \frac{7 \cdot l}{45EI} \end{bmatrix} = \begin{bmatrix} 0 \\ \frac{7}{15} \end{bmatrix} \\
 \begin{bmatrix} M_B \\ M_C \end{bmatrix} &= \begin{bmatrix} \frac{4EI}{2EI} & \frac{2EI}{4EI} \\ \frac{l}{l} & \frac{l}{l} \end{bmatrix} \cdot \begin{bmatrix} \frac{7 \cdot l}{45EI} \\ -\frac{2 \cdot l}{45EI} \end{bmatrix} = \begin{bmatrix} \frac{8}{15} \\ \frac{2}{15} \end{bmatrix} \\
 \begin{bmatrix} M_C \\ M_D \end{bmatrix} &= \begin{bmatrix} \frac{4EI}{2EI} & \frac{2EI}{4EI} \\ \frac{l}{l} & \frac{l}{l} \end{bmatrix} \cdot \begin{bmatrix} -\frac{2 \cdot l}{45EI} \\ \frac{7 \cdot l}{45EI} \end{bmatrix} = \begin{bmatrix} -\frac{2}{15} \\ 0 \end{bmatrix}
 \end{aligned} \tag{B.12}$$

What stands out is the fact the two values for M_B are not the same. This means the value of the moment in the beam is different on each side of the node. This is due to the fact that the load is applied in B. The combined value of the two internal moments equals $\frac{7}{15} + \frac{8}{15} = 1$ This moment counteracts the applied torque, which also has a value of 1. This means the sum of moments on that node equals 0, which is what we would expect. Now all the variables we needed to determine are known. This is the end of the second step in SCIA. What we have done above is again a simplification of what happens in reality. The matrix and vectors will be much larger, but also other things may vary. Adding a fixed support for instance makes the applied torque in that node a variable, while keeping the rotation fixed at 0. However, the general concept of how an input file is converted into usable results remains unchanged. All the results are ultimately collected in an output file.

B.4 GUI

Now the main calculation is done, the third and final step is to display the results in the Graphical User Interface, the GUI. During this step, some additional calculations are performed on the results. To check whether a structure doesn't exceed the maximum allowed deflections or stresses, unity checks are performed. Safety factors and load combinations are collected and reported. The maximum stresses in the cross sections can also be computed, now the internal forces in the elements are known. SCIA also has the ability to draw the structure in deformed state, even in 3D. All this is done with the values obtained by the calculation in the Kernel.

Maple Files for framework analysis of simple portal structure

```

> restart;
> with(linalg):
First the individual flexibility matrices are generated for each element, as well as the vectors with rotations and external moments. Also an empty 4x4
matrix is generated.
> for i from 1 to 3 do
  k[i] :=  $\frac{EI}{l} \cdot (4, 2|2, 4)$ 
end do

```

$$k_1 := \begin{bmatrix} \frac{4EI}{l} & \frac{2EI}{l} \\ \frac{2EI}{l} & \frac{4EI}{l} \end{bmatrix}$$

$$k_2 := \begin{bmatrix} \frac{4EI}{l} & \frac{2EI}{l} \\ \frac{2EI}{l} & \frac{4EI}{l} \end{bmatrix}$$

$$k_3 := \begin{bmatrix} \frac{4EI}{l} & \frac{2EI}{l} \\ \frac{2EI}{l} & \frac{4EI}{l} \end{bmatrix} \tag{1}$$

```

> x, b, A := Vector(4, symbol = varphi), Vector(4, symbol = T), Matrix(4, 4, fill = 0);

```

$$x, b, A := \begin{bmatrix} \varphi_1 \\ \varphi_2 \\ \varphi_3 \\ \varphi_4 \end{bmatrix}, \begin{bmatrix} T_1 \\ T_2 \\ T_3 \\ T_4 \end{bmatrix}, \begin{bmatrix} 0 & 0 & 0 & 0 \\ 0 & 0 & 0 & 0 \\ 0 & 0 & 0 & 0 \\ 0 & 0 & 0 & 0 \end{bmatrix} \tag{2}$$

Figure B.5: 1

```

We assemble the governing flexibility matrix A from the k-matrices of the individual elements, and obtain the following system of equations:
> for i from 1 to 3 do
  A[i..i + 1, i..i + 1] := A[i..i + 1, i..i + 1] + k[i]:
end do:
> print(b = A, x)

```

$$\begin{bmatrix} T_1 \\ T_2 \\ T_3 \\ T_4 \end{bmatrix} = \begin{bmatrix} \frac{4EI}{l} & \frac{2EI}{l} & 0 & 0 \\ \frac{2EI}{l} & \frac{8EI}{l} & \frac{2EI}{l} & 0 \\ 0 & \frac{2EI}{l} & \frac{8EI}{l} & \frac{2EI}{l} \\ 0 & 0 & \frac{2EI}{l} & \frac{4EI}{l} \end{bmatrix} \cdot \begin{bmatrix} \varphi_1 \\ \varphi_2 \\ \varphi_3 \\ \varphi_4 \end{bmatrix} \tag{3}$$

```

> T[1], T[2], T[3], T[4] := 0, 1, 0, 0

```

$$T_1, T_2, T_3, T_4 := 0, 1, 0, 0 \tag{4}$$

```

The system is solved for phi and the solution is obtained in terms of the moments.
> for i from 1 to 4 do
  assign(x[i] = insolve(A, b)[i])
end do
> print(varphi = x)

```

$$\varphi = \begin{bmatrix} -\frac{7}{90} \frac{l}{EI} \\ \frac{7}{45} \frac{l}{EI} \\ -\frac{2}{45} \frac{l}{EI} \\ \frac{1}{45} \frac{l}{EI} \end{bmatrix} \tag{5}$$

Figure B.6: 2

Now we found the rotations, they can be substituted back into the flexibility relations to find the corresponding moments

```
>  
>  
> for i from 1 to 3 do  
  phi[i] := (x[i], x[i + 1]):  
  m[i] := k[i]phi[i]  
end do
```

$$\phi_1 := \begin{bmatrix} -\frac{7}{90} \frac{l}{EI} \\ \frac{7}{45} \frac{l}{EI} \end{bmatrix}$$

$$m_1 := \begin{bmatrix} 0 \\ \frac{7}{15} \end{bmatrix}$$

$$\phi_2 := \begin{bmatrix} \frac{7}{45} \frac{l}{EI} \\ -\frac{2}{45} \frac{l}{EI} \end{bmatrix}$$

$$m_2 := \begin{bmatrix} \frac{8}{15} \\ \frac{2}{15} \end{bmatrix}$$

$$\phi_3 := \begin{bmatrix} -\frac{2}{45} \frac{l}{EI} \\ \frac{1}{45} \frac{l}{EI} \end{bmatrix}$$

$$m_3 := \begin{bmatrix} -\frac{2}{15} \\ 0 \end{bmatrix}$$

(6)

Figure B.7: 3

Appendix C

Maple Files

C.1 Cross sectional properties

> restart;

I-shaped

> $h, b, t := 250.\text{mm}, 200.\text{mm}, 10.\text{mm}$

$$h, b, t := 250.\text{ mm}, 200.\text{ mm}, 10.\text{ mm} \quad (1)$$

Part I:

> $A := 2 \cdot b \cdot t + (h - 2 \cdot t) \cdot t$

$$A := 6300.\text{ mm}^2 \quad (2)$$

> $ync := \frac{\left(\frac{2 \cdot b \cdot t \cdot b}{2} + \frac{(h - 2 \cdot t) \cdot t \cdot b}{2} \right)}{A}$

$$ync := 100.0000000\text{ mm} \quad (3)$$

> $znc := \frac{\left(\frac{b \cdot t \cdot t}{2} + \frac{(h - 2 \cdot t) \cdot t \cdot h}{2} + b \cdot t \cdot \left(h - \frac{t}{2} \right) \right)}{A}$

$$znc := 125.0000000\text{ mm} \quad (4)$$

> $Iyy := 2 \cdot \left(\frac{1}{12} \cdot t \cdot b^3 \right) + \frac{1}{12} \cdot (h - 2 \cdot t) \cdot t^3$

$$Iyy := 1.335250000 \cdot 10^7\text{ mm}^4 \quad (5)$$

> $Izz := \frac{1}{12} \cdot t \cdot (h - 2 \cdot t)^3 + 2 \cdot \left(\frac{1}{12} \cdot b \cdot t^3 + b \cdot t \cdot \left(\frac{h}{2} - \frac{t}{2} \right)^2 \right)$

$$Izz := 6.777250000 \cdot 10^7\text{ mm}^4 \quad (6)$$

> $Iyz := b \cdot t \cdot znc + (h - 2 \cdot t) \cdot t \cdot 0 \cdot 0 + b \cdot t \cdot (-znc)$

$$Iyz := 0. \quad (7)$$

Part II:

> $It := \frac{1}{3} \cdot (h - t) \cdot t^3 + \frac{2}{3} \cdot b \cdot t^3$

$$It := 2.133333333 \cdot 10^5\text{ mm}^4 \quad (8)$$

> shear centre eccentricity:

> $dy, dz := 0, 0$

$$dy, dz := 0, 0 \quad (9)$$

L-shaped

> restart;

> $h, b, t := 250.\text{mm}, 250.\text{mm}, 25.\text{mm}$

$$h, b, t := 250.\text{ mm}, 250.\text{ mm}, 25.\text{ mm} \quad (10)$$

Part I:

> $A := h \cdot t + (b - t) \cdot t$

$$A := 11875.\text{ mm}^2 \quad (11)$$

> $ync := \frac{\left(\frac{h \cdot t \cdot t}{2} + (b - t) \cdot t \cdot \left(\frac{(b - t)}{2} + t \right) \right)}{A}$

$$ync := 71.71052632\text{ mm} \quad (12)$$

$$\begin{aligned} > z_{nc} := \frac{\left(\frac{h \cdot t \cdot h}{2} + \frac{(b-t) \cdot t \cdot t}{2} \right)}{A} \\ & z_{nc} := 71.71052632 \text{ mm} \end{aligned} \quad (13)$$

$$\begin{aligned} > I_{yy} := \frac{1}{12} \cdot h \cdot t^3 + h \cdot t \cdot \left(y_{nc} - \frac{t}{2} \right)^2 + \frac{1}{12} \cdot t \cdot (b-t)^3 + (b-t) \cdot t \cdot \left(\frac{(b-t)}{2} + t - y_{nc} \right)^2 \\ & I_{yy} := 7.031421326 \cdot 10^7 \text{ mm}^4 \end{aligned} \quad (14)$$

$$\begin{aligned} > I_{zz} := \frac{1}{12} \cdot t \cdot h^3 + h \cdot t \cdot \left(\frac{h}{2} - z_{nc} \right)^2 + \frac{1}{12} \cdot (b-t) \cdot t^3 + (b-t) \cdot t \cdot \left(z_{nc} - \frac{t}{2} \right)^2 \\ & I_{zz} := 7.031421326 \cdot 10^7 \text{ mm}^4 \end{aligned} \quad (15)$$

$$\begin{aligned} > I_{yz} := h \cdot t \cdot \left(- \left(y_{nc} - \frac{t}{2} \right) \right) \cdot \left(\frac{h}{2} - z_{nc} \right) + (b-t) \cdot t \cdot \left(\frac{(b-t)}{2} + t - y_{nc} \right) \cdot \left(- \left(z_{nc} - \frac{t}{2} \right) \right) \\ & I_{yz} := -4.163240131 \cdot 10^7 \text{ mm}^4 \end{aligned} \quad (16)$$

Part II:

$$\begin{aligned} > I_t := \frac{1}{3} \cdot h \cdot t^3 + \frac{1}{3} \cdot (b-t) \cdot t^3 \\ & I_t := 2.473958333 \cdot 10^6 \text{ mm}^4 \end{aligned} \quad (17)$$

Shear centre eccentricity in local coordinate system:

$$\begin{aligned} > \langle dy[loc], dz[loc] \rangle &:= \left\langle y_{nc} - \frac{t}{2}, z_{nc} - \frac{t}{2} \right\rangle \\ & \langle dy_{loc} \ dz_{loc} \rangle := \begin{bmatrix} 59.21052632 \text{ mm} \\ 59.21052632 \text{ mm} \end{bmatrix} \end{aligned} \quad (18)$$

Shear centre eccentricity in principal coordinate system:

$$\begin{aligned} > \alpha &:= \frac{\text{Pi}}{4} \\ & \alpha := \frac{1}{4} \pi \end{aligned} \quad (19)$$

$$> \langle dy[pri], dz[pri] \rangle := \text{evalf}(\langle \cos(\alpha), -\sin(\alpha) | \sin(\alpha), \cos(\alpha) \rangle \cdot \langle dy[loc], dz[loc] \rangle)$$

$$\langle dy_{pri} \ dz_{pri} \rangle := \begin{bmatrix} 83.73632933 \text{ mm} \\ 0. \end{bmatrix} \quad (20)$$

>

C.2 L-shaped cross section loaded in pure bending

```
> restart;
> with(linalg) :
```

Loading:

```
> m[y] := 0
```

$$m_y := 0 \quad (1)$$

```
> m[z] := 5e6·N·mm
```

$$m_z := 5 \cdot 10^6 \text{ N mm} \quad (2)$$

Cross sectional properties:

```
> l := 5000·mm
```

$$l := 5000 \text{ mm} \quad (3)$$

```
> Iyy := 7.031421326e7 ·mm4
```

$$I_{yy} := 7.031421326 \cdot 10^7 \text{ mm}^4 \quad (4)$$

```
> Izz := 7.031421326e7 ·mm4
```

$$I_{zz} := 7.031421326 \cdot 10^7 \text{ mm}^4 \quad (5)$$

```
> Iyz := -4.163240131e7 ·mm4
```

$$I_{yz} := -4.163240131 \cdot 10^7 \text{ mm}^4 \quad (6)$$

```
> E :=  $\frac{210e3 \cdot N}{mm^2}$ 
```

$$E := \frac{2.10 \cdot 10^5 \text{ N}}{mm^2} \quad (7)$$

```
> EI := evalf(⟨E·Iyy, E·Iyz|E·Iyz, E·Izz⟩)
```

$$EI := \begin{bmatrix} 1.476598478 \cdot 10^{13} \text{ N mm}^2 & -8.742804275 \cdot 10^{12} \text{ N mm}^2 \\ -8.742804275 \cdot 10^{12} \text{ N mm}^2 & 1.476598478 \cdot 10^{13} \text{ N mm}^2 \end{bmatrix} \quad (8)$$

```
> M := ⟨m[y], m[z]⟩
```

$$M := \begin{bmatrix} 0 \\ 5 \cdot 10^6 \text{ N mm} \end{bmatrix} \quad (9)$$

```
> K := ⟨kappa[y], kappa[z]⟩
```

$$K := \begin{bmatrix} \kappa_y \\ \kappa_z \end{bmatrix} \quad (10)$$

```
> assign(K[1] = (inverse(EI).M) [1])
> assign(K[2] = (inverse(EI).M) [2])
> K
```

$$\begin{bmatrix} \frac{3.087198986 \cdot 10^{-7}}{mm} \\ \frac{5.214063110 \cdot 10^{-7}}{mm} \end{bmatrix} \quad (11)$$

Finding displacements using curvature distribution:

> $U := \langle u[y], u[z] \rangle :$

> $u[y] := \frac{\text{kappa}[y] \cdot l \cdot l}{2}$

$u_y := 3.858998732 \text{ mm}$

(12)

> $u[z] := \frac{\text{kappa}[z] \cdot l \cdot l}{2}$

$u_z := 6.517578890 \text{ mm}$

(13)

>

C.3 L-shaped cross section loaded in normal force centre

```
> restart;
> with(linalg) :
```

Input:

```
> E :=  $\frac{210e3 \cdot N}{mm^2}$ 
```

$$E := \frac{2.10 \cdot 10^5 N}{mm^2} \quad (1)$$

```
> G :=  $\frac{8.1e4 \cdot N}{mm^2}$ 
```

$$G := \frac{81000. N}{mm^2} \quad (2)$$

```
> F := 10e3 · N
```

$$F := 10000. N \quad (3)$$

```
> l := 5000 · mm
```

$$l := 5000 mm \quad (4)$$

```
> d[y] := 59.21 · mm
```

$$d_y := 59.21 mm \quad (5)$$

Loading:

```
> m[y] := 0
```

$$m_y := 0 \quad (6)$$

```
> m[z] := F · l
```

$$m_z := 5.0000 \cdot 10^7 N mm \quad (7)$$

```
> m[x] := F · d[y]
```

$$m_x := 5.9210 \cdot 10^5 N mm \quad (8)$$

Cross sectional properties:

```
>
```

```
> Iyy := 7.031421326e7 · mm4
```

$$I_{yy} := 7.031421326 \cdot 10^7 mm^4 \quad (9)$$

```
> Izz := 7.031421326e7 · mm4
```

$$I_{zz} := 7.031421326 \cdot 10^7 mm^4 \quad (10)$$

```
> Iyz := -4.163240131e7 · mm4
```

$$I_{yz} := -4.163240131 \cdot 10^7 mm^4 \quad (11)$$

```
> It := 2.473958333e6 · mm4
```

$$I_t := 2.473958333 \cdot 10^6 mm^4 \quad (12)$$

```
> EI := evalf(⟨E·Iyy, E·Iyz|E·Iyz, E·Izz⟩)
```

$$EI := \begin{bmatrix} 1.476598478 \cdot 10^{13} N mm^2 & -8.742804275 \cdot 10^{12} N mm^2 \\ -8.742804275 \cdot 10^{12} N mm^2 & 1.476598478 \cdot 10^{13} N mm^2 \end{bmatrix} \quad (13)$$

```
> M := ⟨m[y], m[z]⟩
```

$$M := \begin{bmatrix} 0 \\ 5.0000 \cdot 10^7 \text{ N mm} \end{bmatrix} \quad (14)$$

> $K := \langle \text{kappa}[y], \text{kappa}[z] \rangle$

$$K := \begin{bmatrix} \kappa_y \\ \kappa_z \end{bmatrix} \quad (15)$$

> $\text{assign}(K[1] = (\text{inverse}(EI) \cdot M) [1])$

> $\text{assign}(K[2] = (\text{inverse}(EI) \cdot M) [2])$

> K

$$\begin{bmatrix} \frac{0.000003087198986}{\text{mm}} \\ \frac{0.000005214063110}{\text{mm}} \end{bmatrix} \quad (16)$$

Finding displacements using curvature distribution:

> $U := \langle u[y], u[z] \rangle :$

> $u[y] := \frac{\text{kappa}[y] \cdot 0.5 \cdot l \cdot 2 \cdot l}{3}$

$$u_y := 25.72665822 \text{ mm} \quad (17)$$

> $u[z] := \frac{\text{kappa}[z] \cdot 0.5 \cdot l \cdot 2 \cdot l}{3}$

$$u_z := 43.45052590 \text{ mm} \quad (18)$$

> $\text{varphi}[x] := \frac{m[x] \cdot l}{G \cdot It} \cdot 1000 \cdot \text{mrad}$

$$\varphi_x := 14.77364523 \text{ mrad} \quad (19)$$

>